Path Integral Monte Carlo Simulations of Warm Dense Matter

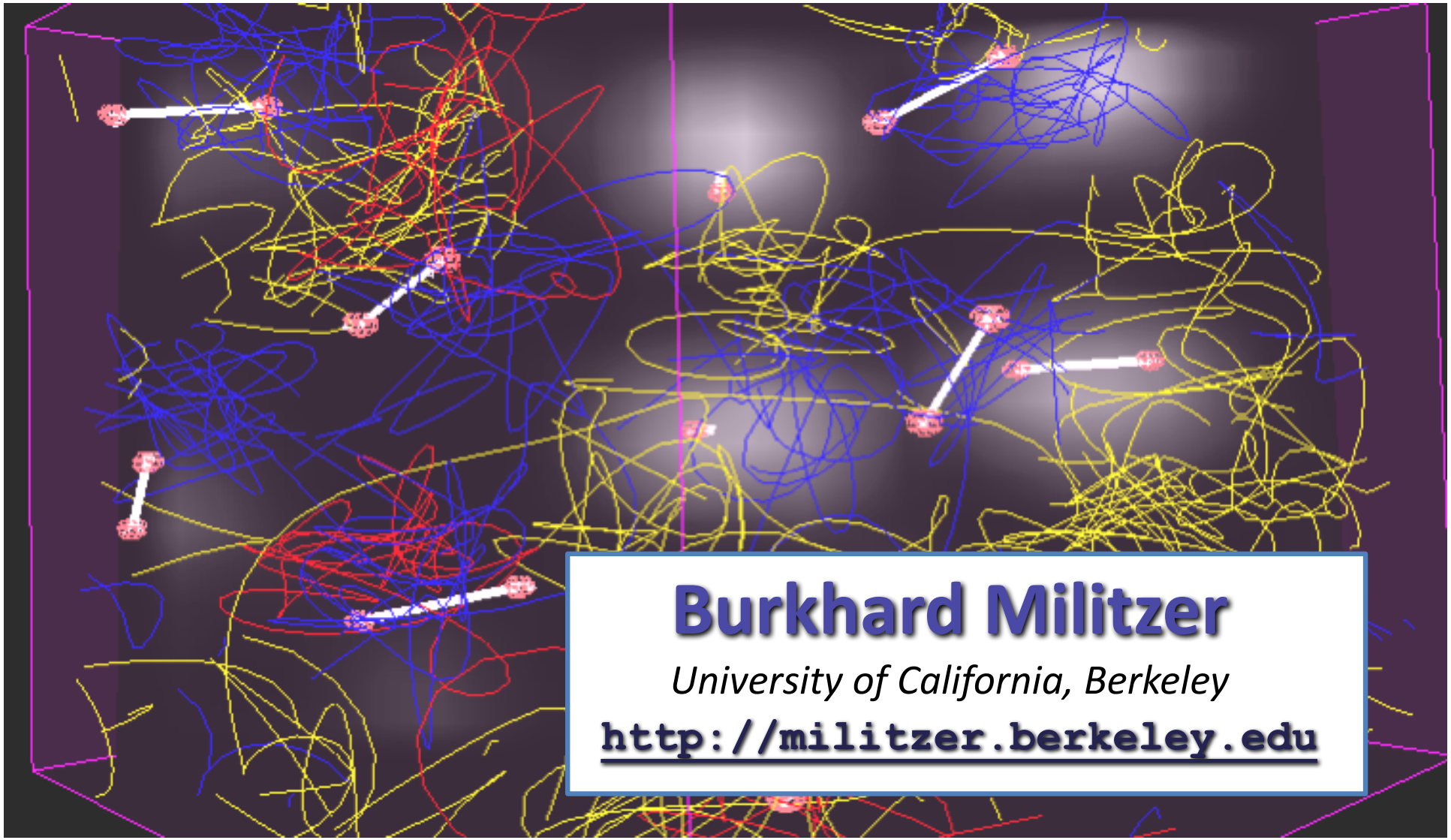

Burkhard Militzer

University of California, Berkeley

http://militzer.berkeley.edu

Outline

1. **Path integral Monte Carlo simulation method**
2. **Application of CH plastic ablator materials**
3. **Application to warm, dense silicon**

Kevin Driver, Francois Soubiran, Shuai Zhang

Lorin Benedict (LLNL) and Suxing Hu (LLE)

Supported by NSF-DOE partnership for plasma science. PRAC computer time on Bluewaters machine at Urbana-Champaign, IL.

Two postdoc positions to be filled in Aug. 2018

Phase Diagram of Hydrogen

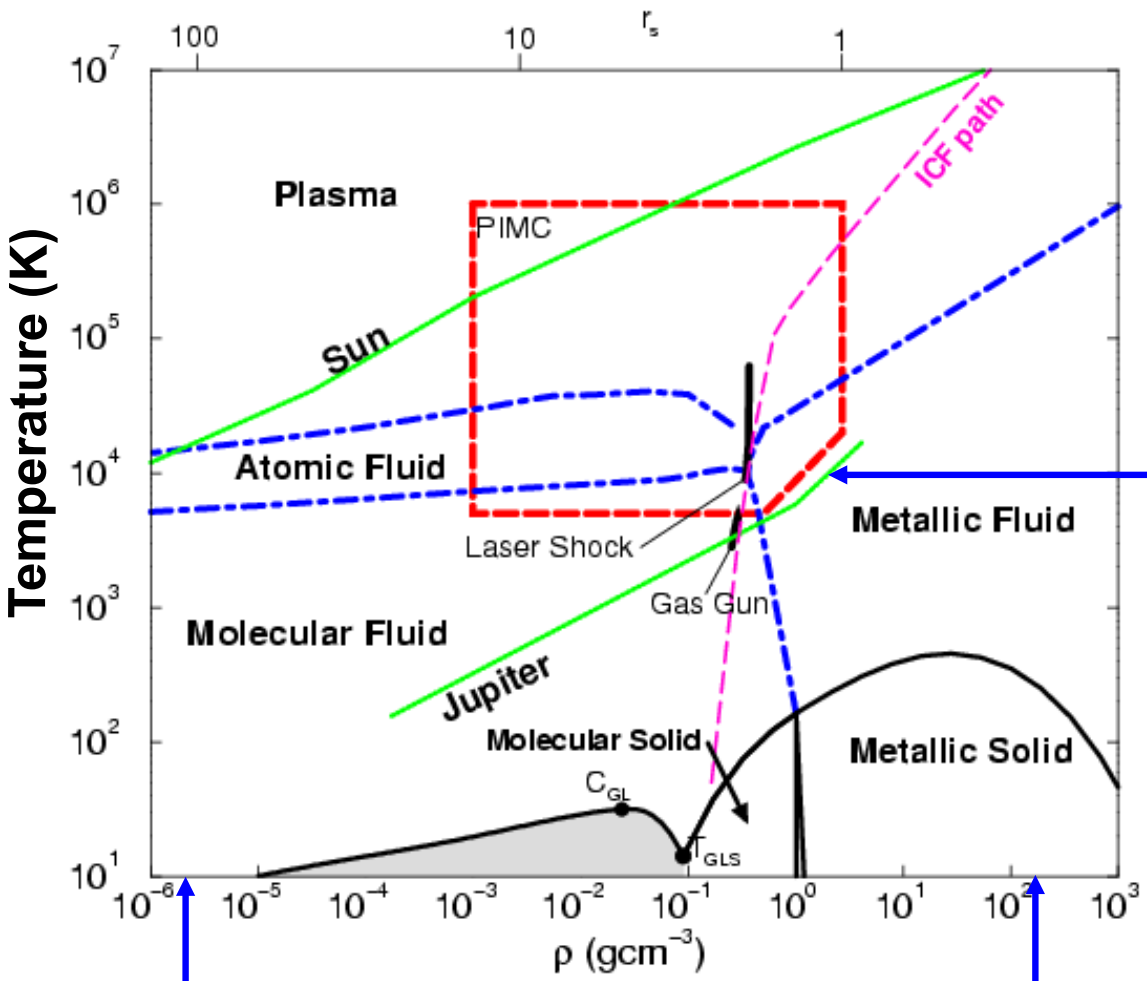

Solar GP: Jupiter, Saturn

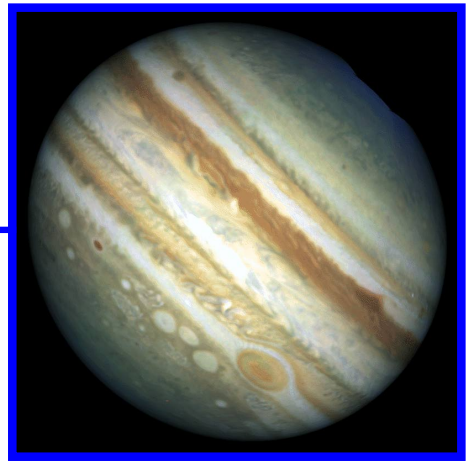

$n=10^{18}$ cm^{-3}

Density

$n=10^{26}$ cm^{-3}

1) Path integral Monte Carlo for T>5000K

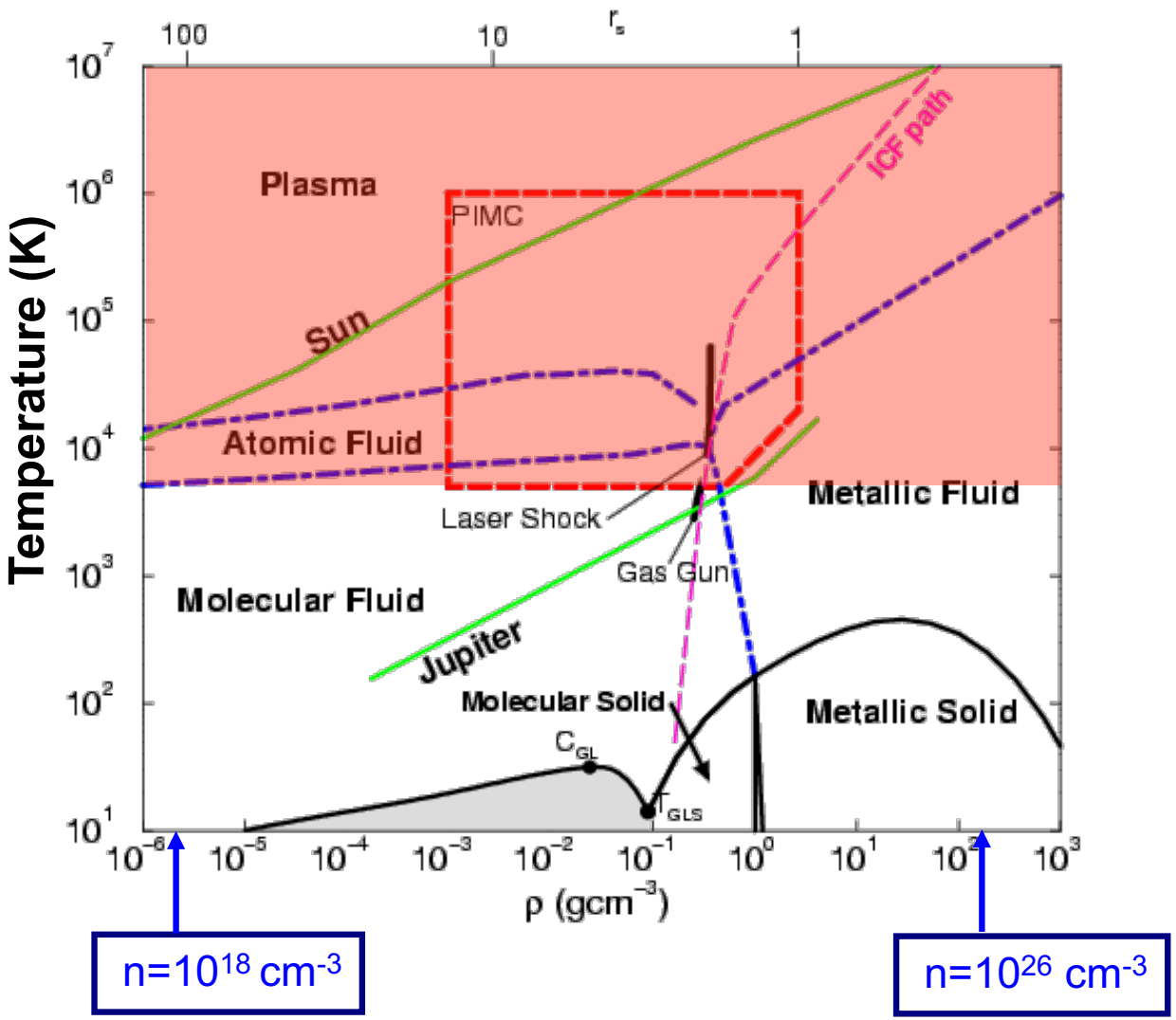

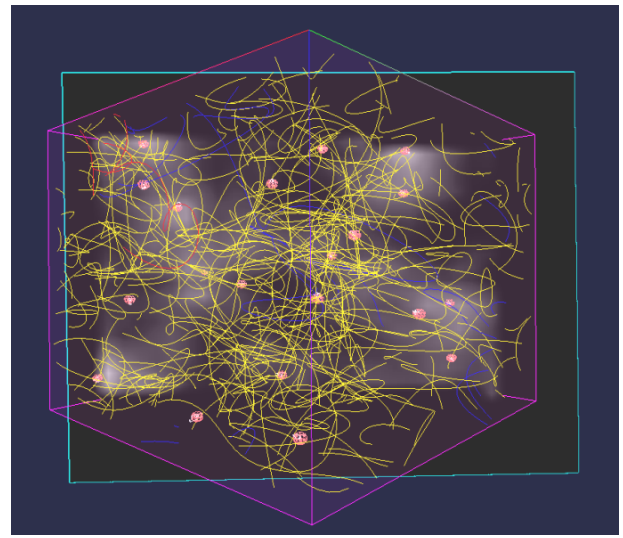

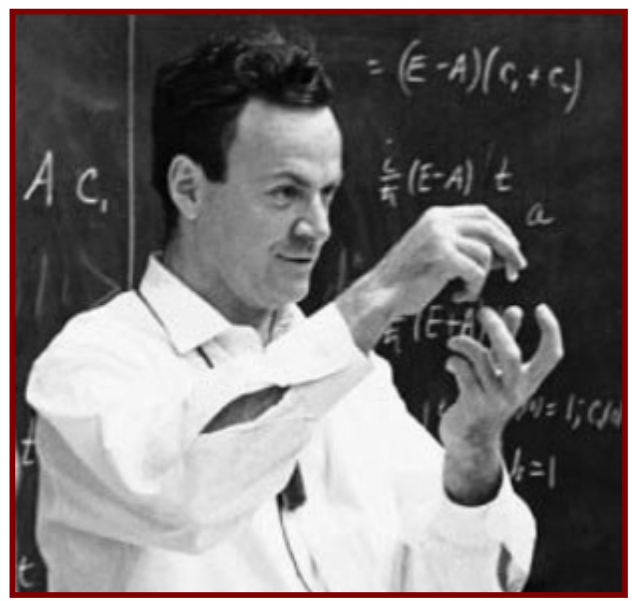

1) Path integral Monte Carlo for T>5000K
2) Density functional molecular dynamics below

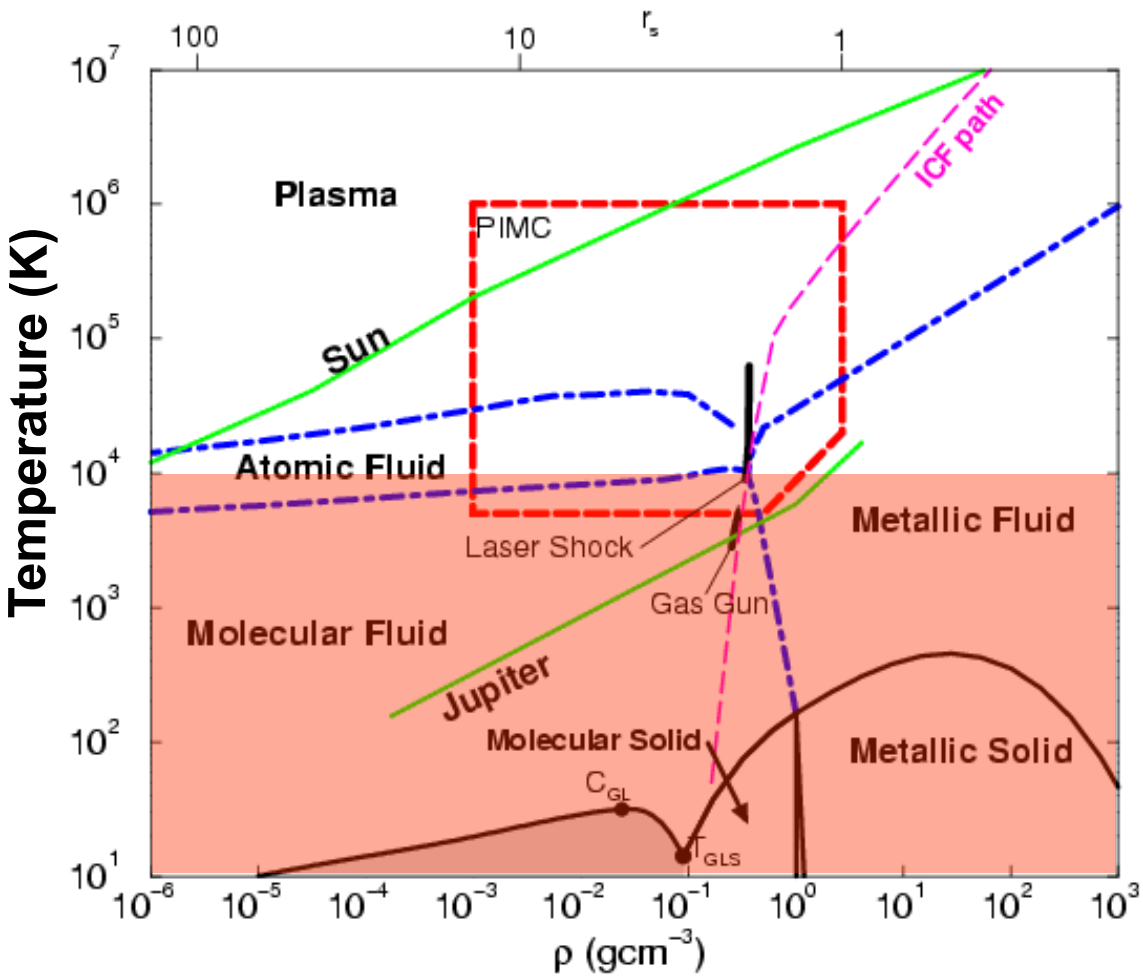

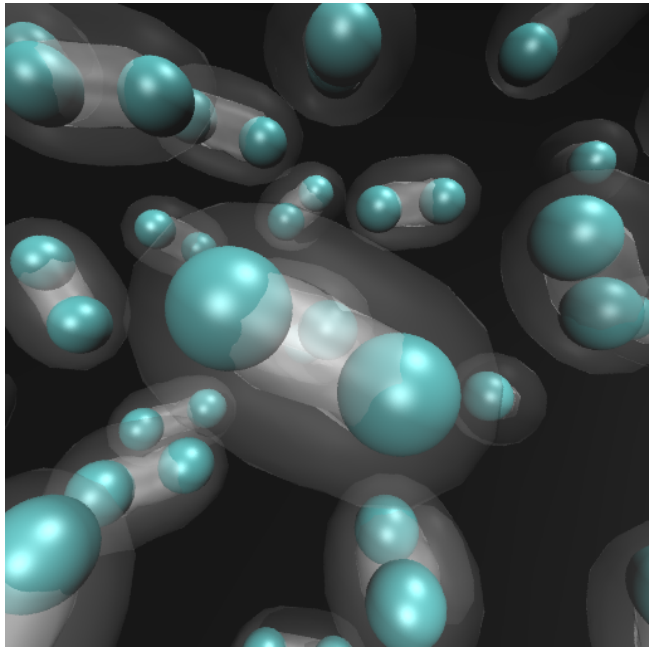

Born-Oppenheimer approx.
MD with classical nuclei:

F = m a

Forces derived DFT with electrons in the instantaneous ground state.

Juno Mission
Now in orbit around Jupiter

- Interior model to match gravity data
- Equation of state calculations for hydrogen-helium mixtures
- Thermodynamics of heavier elements (Z)

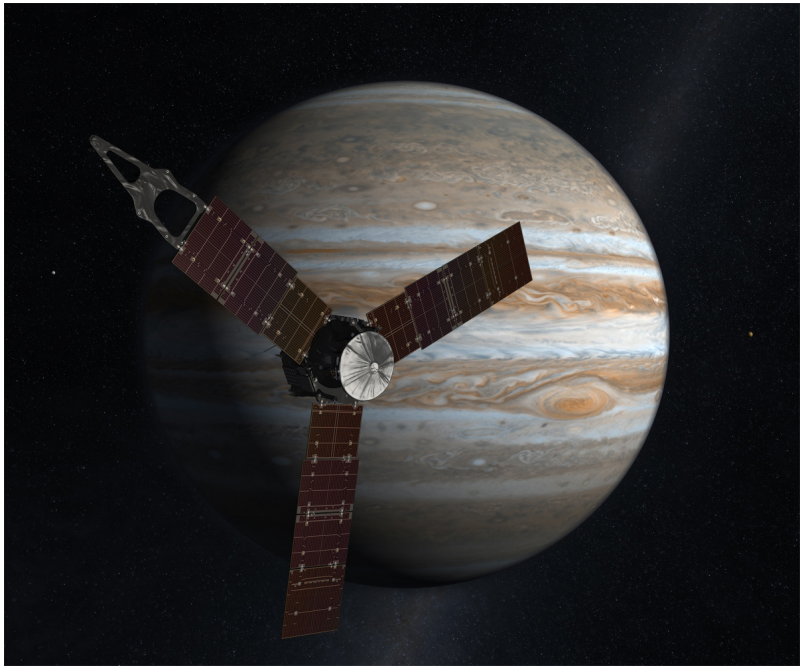

Mission Timeline:
- Launch - August 2011
- Earth flyby gravity assist - October 2013
- Jupiter arrived in July 2016
- End of mission much past October 2017

I. Path Integral Monte Carlo

Step 1 towards the path integral

Matrix squaring property of the density matrix

Matrix squaring in operator notation:

$$\hat{\rho} = e^{-\beta \hat{\mathrm{H}}} = \left(e^{-(\beta/2)\hat{\mathrm{H}}}\right)\left(e^{-(\beta/2)\hat{\mathrm{H}}}\right), \quad \beta = \frac{1}{k_B T}$$

Matrix squaring in real-space notation:

$$\langle R | \hat{\rho} | R' \rangle = \int dR_1 \, \langle R | e^{-(\beta/2)\hat{\mathrm{H}}} | R_1 \rangle \, \langle R_1 | e^{-(\beta/2)\hat{\mathrm{H}}} | R' \rangle$$

Matrix squaring in matrix notation:

$$\begin{bmatrix} \cdots & R' & \cdots \\ R & \ddots & \vdots \\ \cdots & \cdots & \cdots \end{bmatrix} = \begin{bmatrix} \cdots & R_1 & \cdots \\ R & \ddots & \vdots \\ \cdots & \cdots & \cdots \end{bmatrix} * \begin{bmatrix} \cdots & R' & \cdots \\ R_1 & \ddots & \vdots \\ \cdots & \cdots & \cdots \end{bmatrix}$$

Repeat the matrix squaring step

Matrix squaring in operator notation:

$$\hat{\rho} = e^{-\beta \hat{\mathrm{H}}} = \left(e^{-(\beta/4)\hat{\mathrm{H}}} \right)^4, \quad \beta = \frac{1}{k_B T}$$

Matrix squaring in real-space notation:

$$\langle R | \hat{\rho} | R' \rangle = \int dR_1 \int dR_2 \int dR_3 \langle R | e^{-(\beta/4)\hat{\mathrm{H}}} | R_1 \rangle \langle R_1 | e^{-(\beta/4)\hat{\mathrm{H}}} | R_2 \rangle \langle R_2 | e^{-(\beta/4)\hat{\mathrm{H}}} | R_3 \rangle \langle R_3 | e^{-(\beta/4)\hat{\mathrm{H}}} | R' \rangle$$

Path Integrals in Imaginary Time

Simplest form for the paths' action: primitive approx.

Density matrix:

$$\hat{\rho} = e^{-\beta \hat{H}} = \left(e^{-\tau \hat{H}}\right)^M, \quad \beta = \frac{1}{k_B T}, \quad \tau = \frac{\beta}{M}$$

$$\langle \hat{O} \rangle = \frac{\mathrm{Tr}[\hat{O}\hat{\rho}]}{\mathrm{Tr}[\hat{\rho}]}$$

M step path integral:

$$\langle R | \hat{\rho} | R' \rangle = \langle R | (e^{-\tau \hat{H}})^M | R' \rangle = \int dR_1 \ldots \int dR_{M-1} \langle R | e^{-\tau \hat{H}} | R_1 \rangle \langle R_1 | e^{-\tau \hat{H}} | R_2 \rangle \ldots \langle R_{M-1} | e^{-\tau \hat{H}} | R' \rangle$$

Path integral and primitive action *S* :

$$\langle R | \hat{\rho} | R' \rangle = \oint_{R \to R'} dR_t e^{-S[R_t]}$$

$$S[R_t] = \sum_{i=1}^{M} \frac{(R_{i+1} - R_i)^2}{4\lambda\tau} + \frac{\tau}{2}\left[V(R_i) + V(R_{i+1})\right]$$

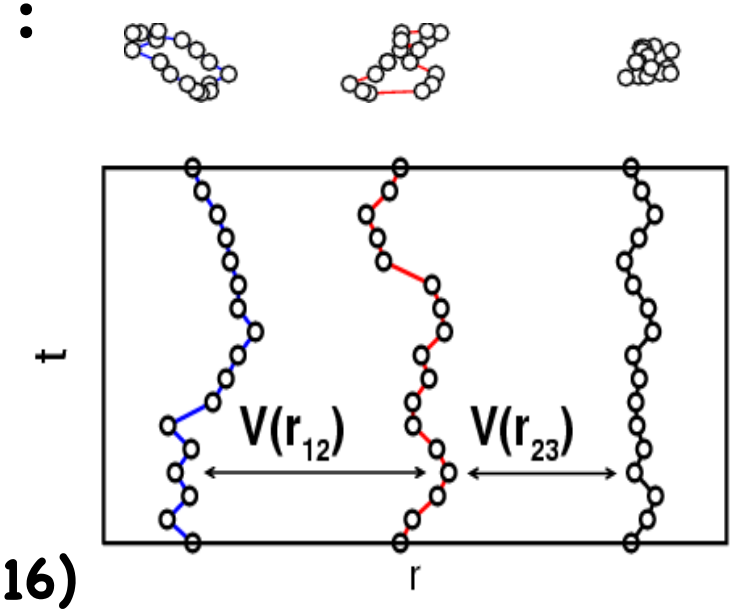

Pair action: Militzer, Comp. Phys. Comm. (2016)

Bosonic and Fermionic Path Integrals

Bosonic density matrix:
Sum over all symmetric eigenstates.

$$\rho_B(R,R',\beta) = \sum_i e^{-\beta\, E_i}\ \Psi_S^{[i]*}(R)\ \Psi_S^{[i]}(R')$$

Fermionic density matrix:
Sum over all antisymmetric eigenstates.

$$\rho_F(R,R',\beta) = \sum_i e^{-\beta\, E_i}\ \Psi_{AS}^{[i]*}(R)\ \Psi_{AS}^{[i]}(R')$$

Project out the symmetric states:

$$\rho_B(R,R',\beta) = \sum_P (+1)^P\ \rho_D(R,PR',\beta)$$

Project out the antisymmetric states:

$$\rho_F(R,R',\beta) = \sum_P (-1)^P\ \rho_D(R,PR',\beta)$$

$$\langle R|\hat{\rho}_{F/B}|R'\rangle = \sum_P (\pm 1)^P \int dR_1 \ldots \int dR_{M-1} \langle R|e^{-\tau\hat{H}}|R_1\rangle \ldots \langle R_{M-1}|e^{-\tau\hat{H}}|PR'\rangle$$

D:

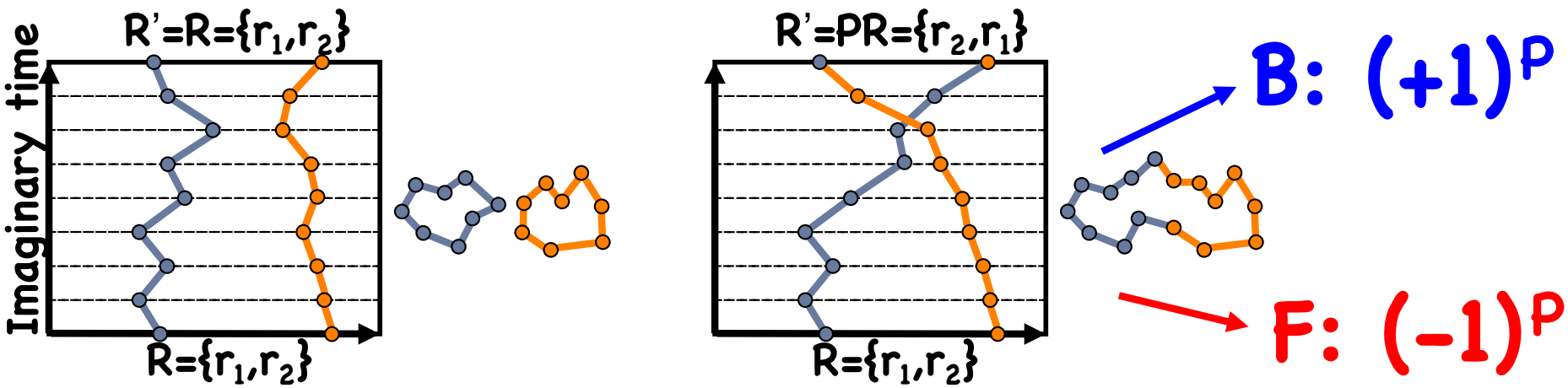

Restricted PIMC for fermions: How is the restriction applied?

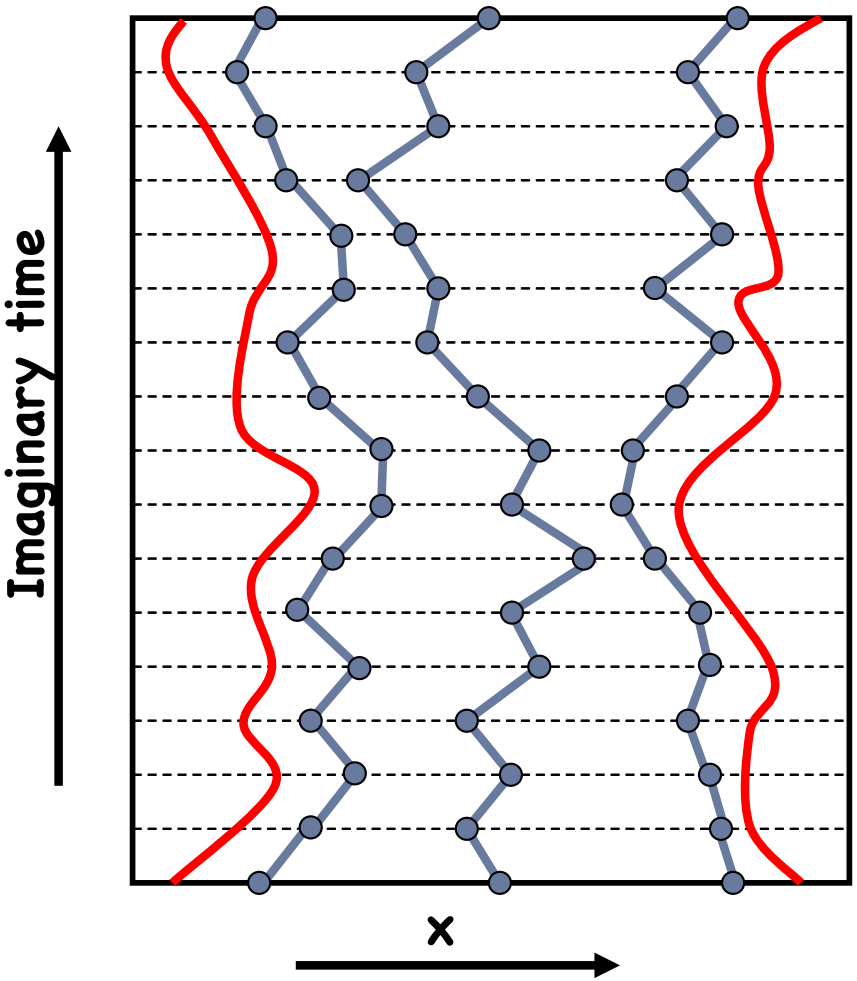

Construct a fermionic trial density matrix in form of a Slater determinant of single-particle density matrices:

$$\rho_T(R,R',\beta) = \begin{vmatrix} \rho(r_1,r_1',\beta) & \cdots & \rho(r_1,r_N',\beta) \\ \vdots & \ddots & \vdots \\ \rho(r_N,r_1',\beta) & \cdots & \rho(r_N,r_N',\beta) \end{vmatrix}$$

Enforce the following nodal condition for all time slices along the paths:

$$\rho_T\left[R(t),R(0),t\right] > 0$$

This 3N-dimensional conditions eliminates all negative and some positive contribution to the path → Solves the fermion sign problem approx.

Free-particle nodes:

$$\rho_0^{[1]}(r,r';\beta) = \sum_k e^{-\beta E_k}\,\Psi_k(r)\,\Psi_k^*(r')$$

Starting from Restricted PIMC Simulations of Hydrogen

PHYSICAL REVIEW LETTERS

VOLUME 73 | 17 OCTOBER 1994 | NUMBER 16

Equation of State of the Hydrogen Plasma by Path Integral Monte Carlo Simulation

C. Pierleoni,[1,2,*] D. M. Ceperley,[3] B. Bernu,[1] and W. R. Magro[3]

VOLUME 76, NUMBER 8 | PHYSICAL REVIEW LETTERS | 19 FEBRUARY 1996

Molecular Dissociation in Hot, Dense Hydrogen

W. R. Magro,[1] D. M. Ceperley,[2] C. Pierleoni,[3] and B. Bernu[4]

PIMC and DFT-MD Simulations of Hydrogen and Helium

Hydrogen

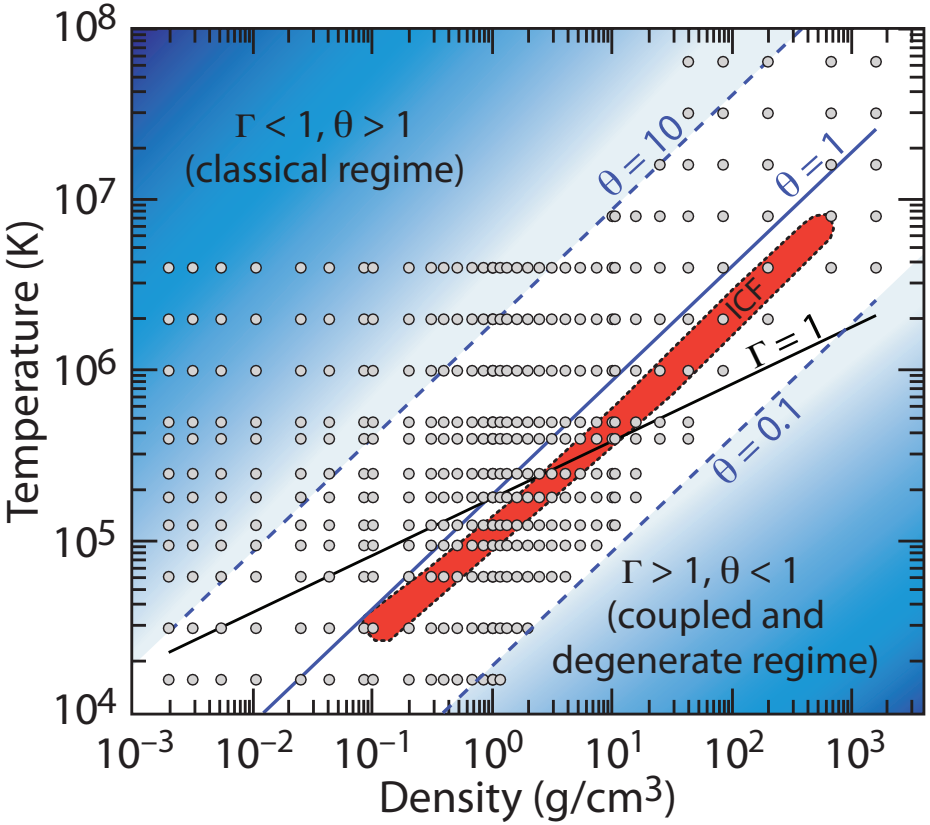

S. X. Hu, B. Militzer, V. N. Goncharov, S. Skupsky, *Phys. Rev. Lett.*, **104** (2010) 235003
Phys. Rev. B **84** (2011) 224109.

Helium

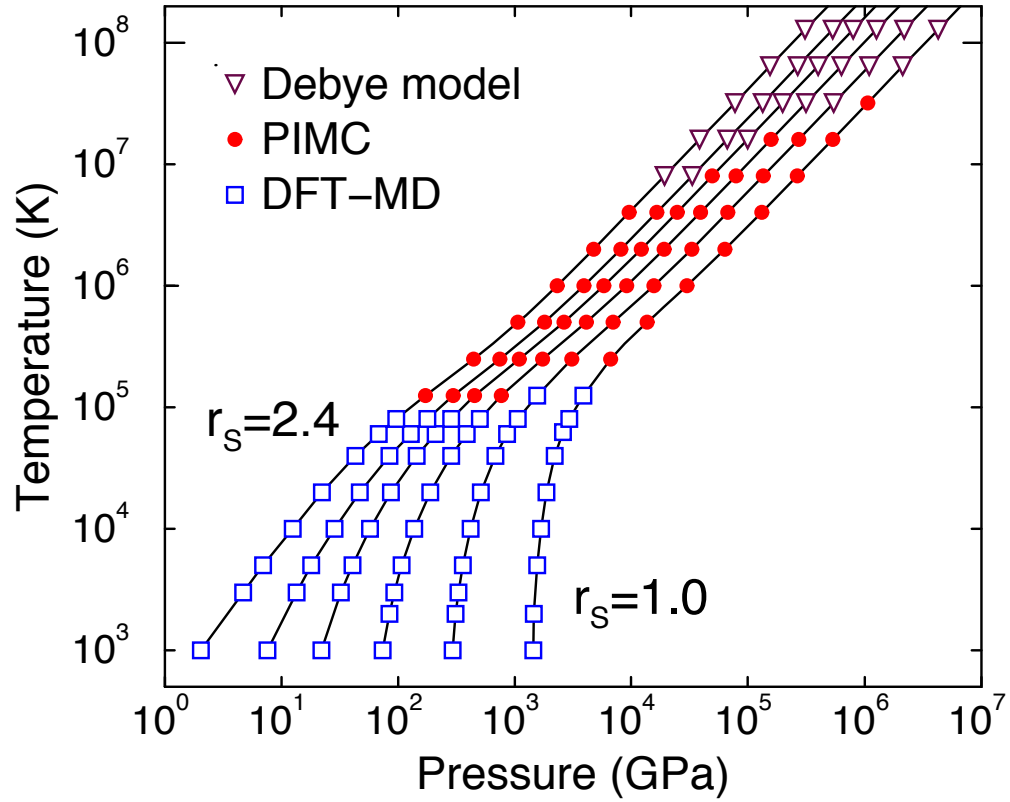

B. Militzer, *Phys. Rev.* B **79** (2009) 155105
B. Militzer, *Phys. Rev. Lett.* **97** (2006) 175501

Water and Carbon

First Path Integral Monte Carlo Simulations for Heavier Elements Fill this Gap in Temperature

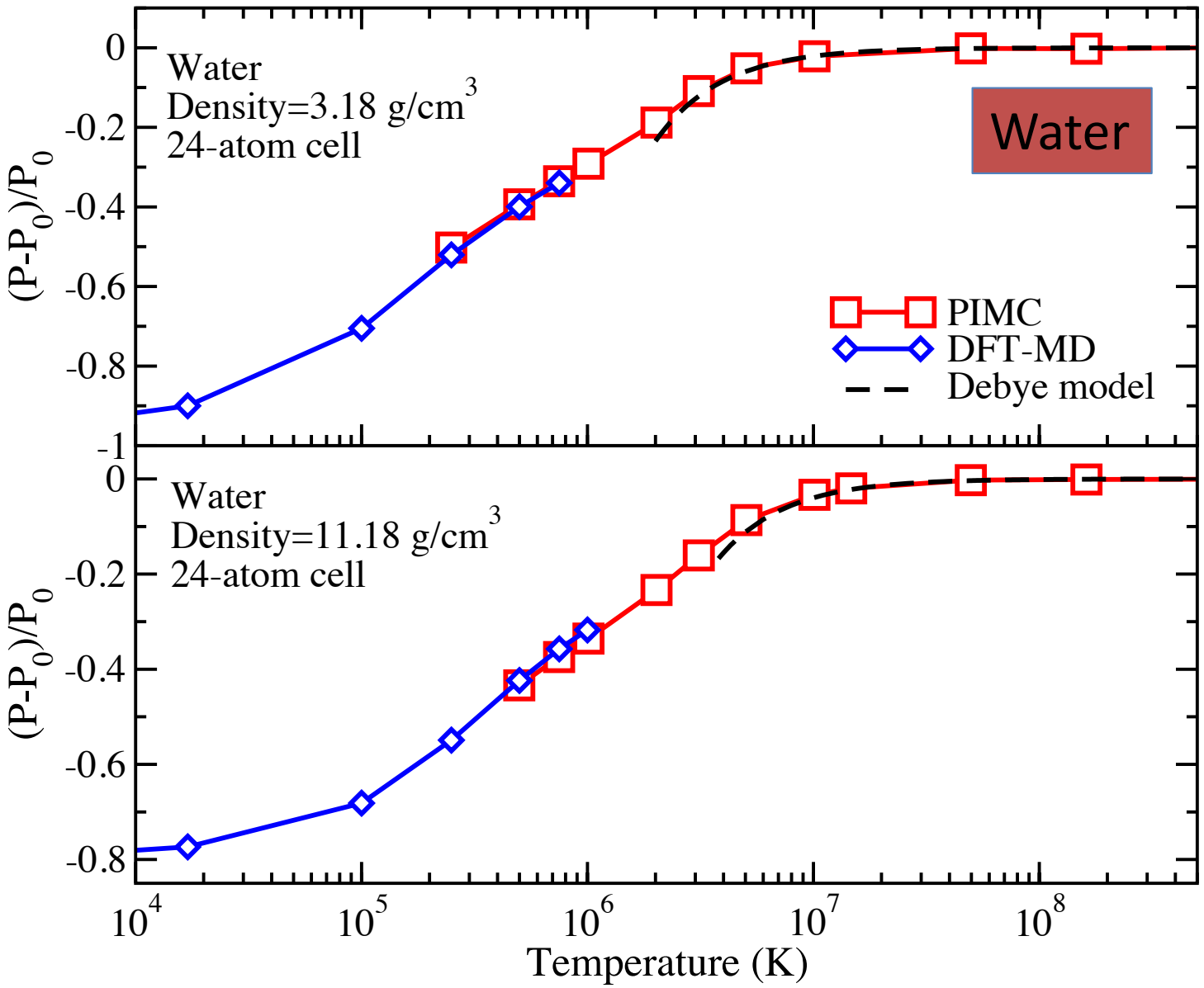

Again Path Integral Monte Carlo bridges the Gap in T between DFT-MD and the Debye Model

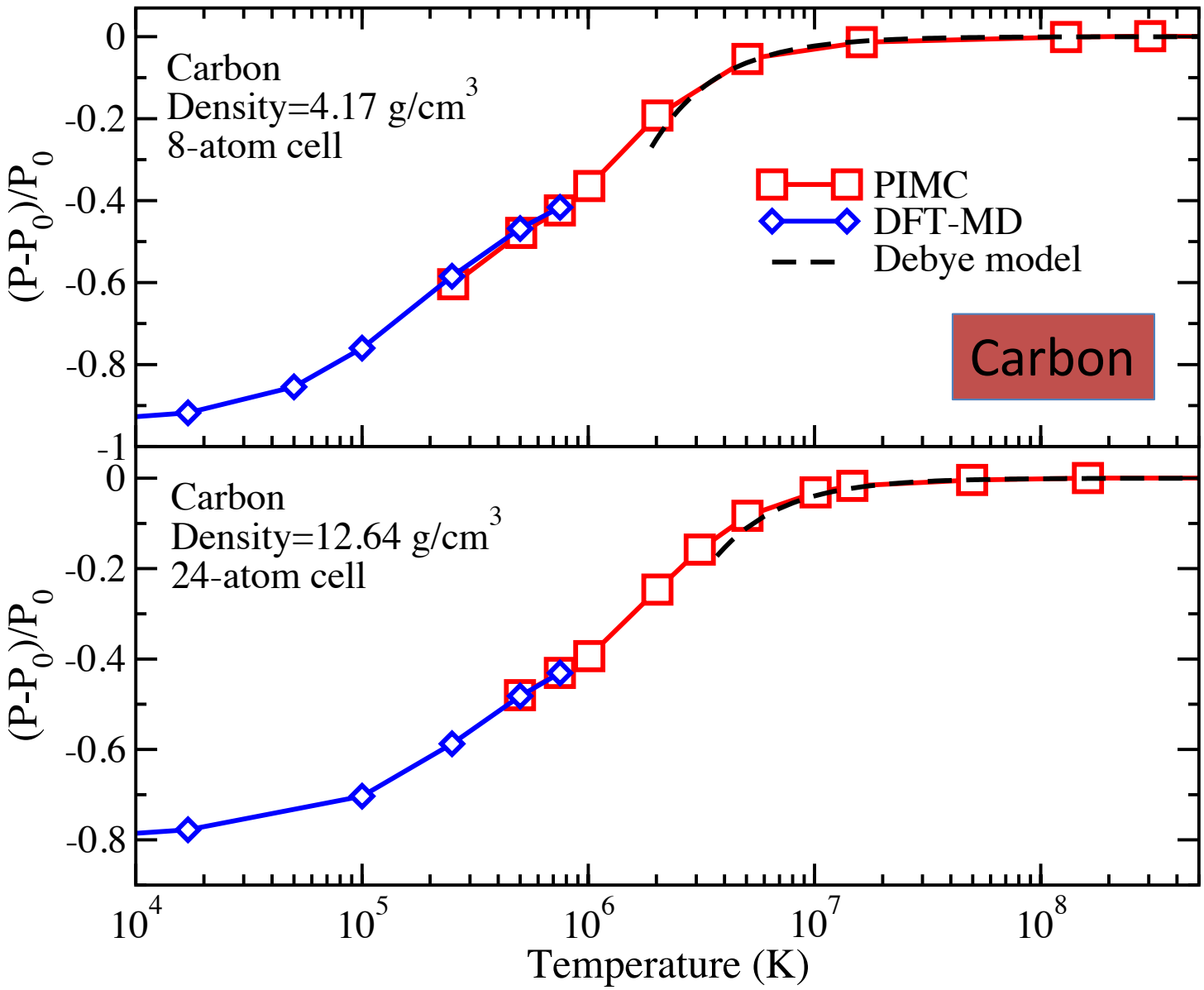

Path Integral Monte Carlo bridges the Gap in Internal Energy vs Temperature for Water and Carbon Plasmas

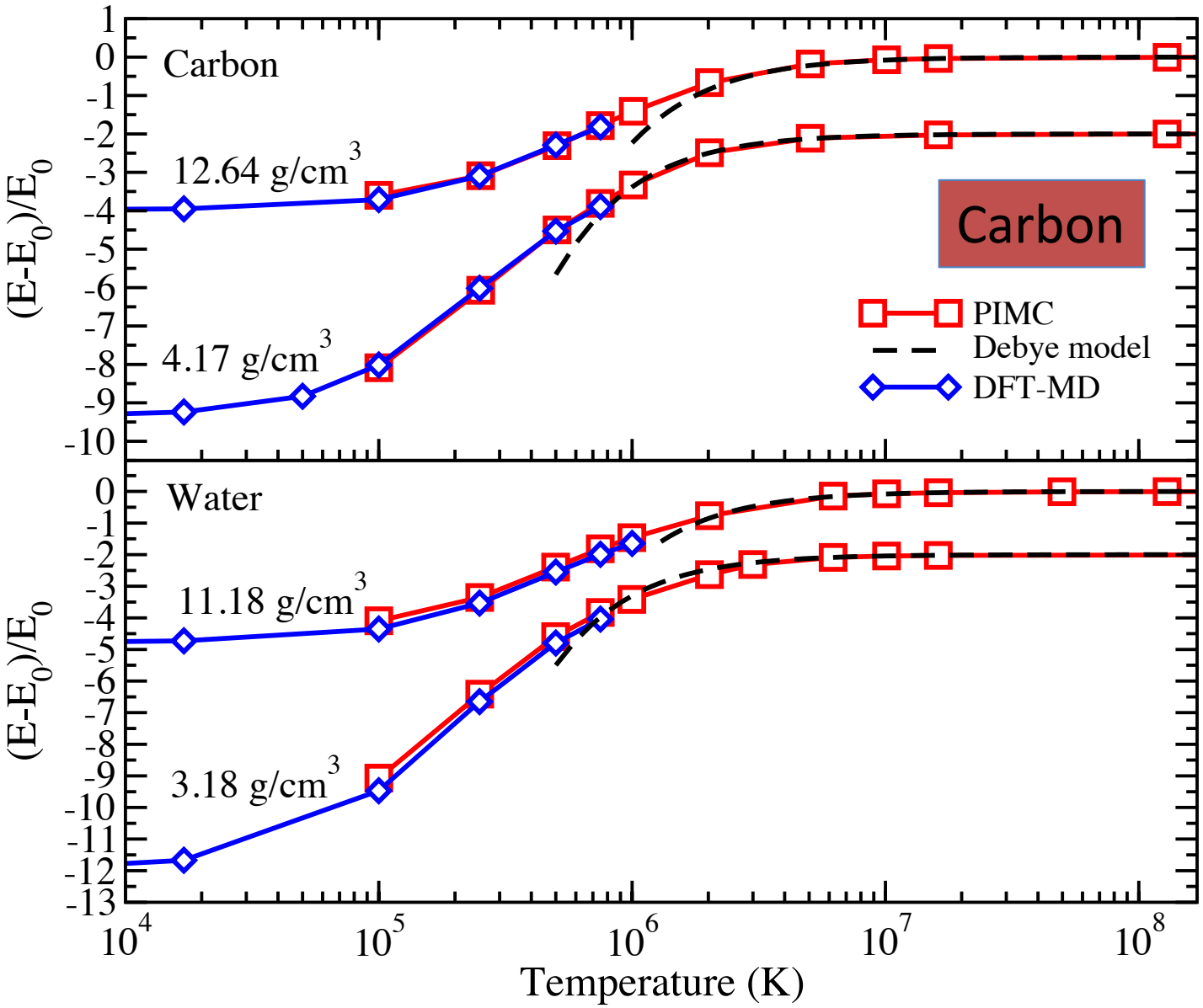

Path Integral Monte Carlo and DFT-MD are in very good agreement

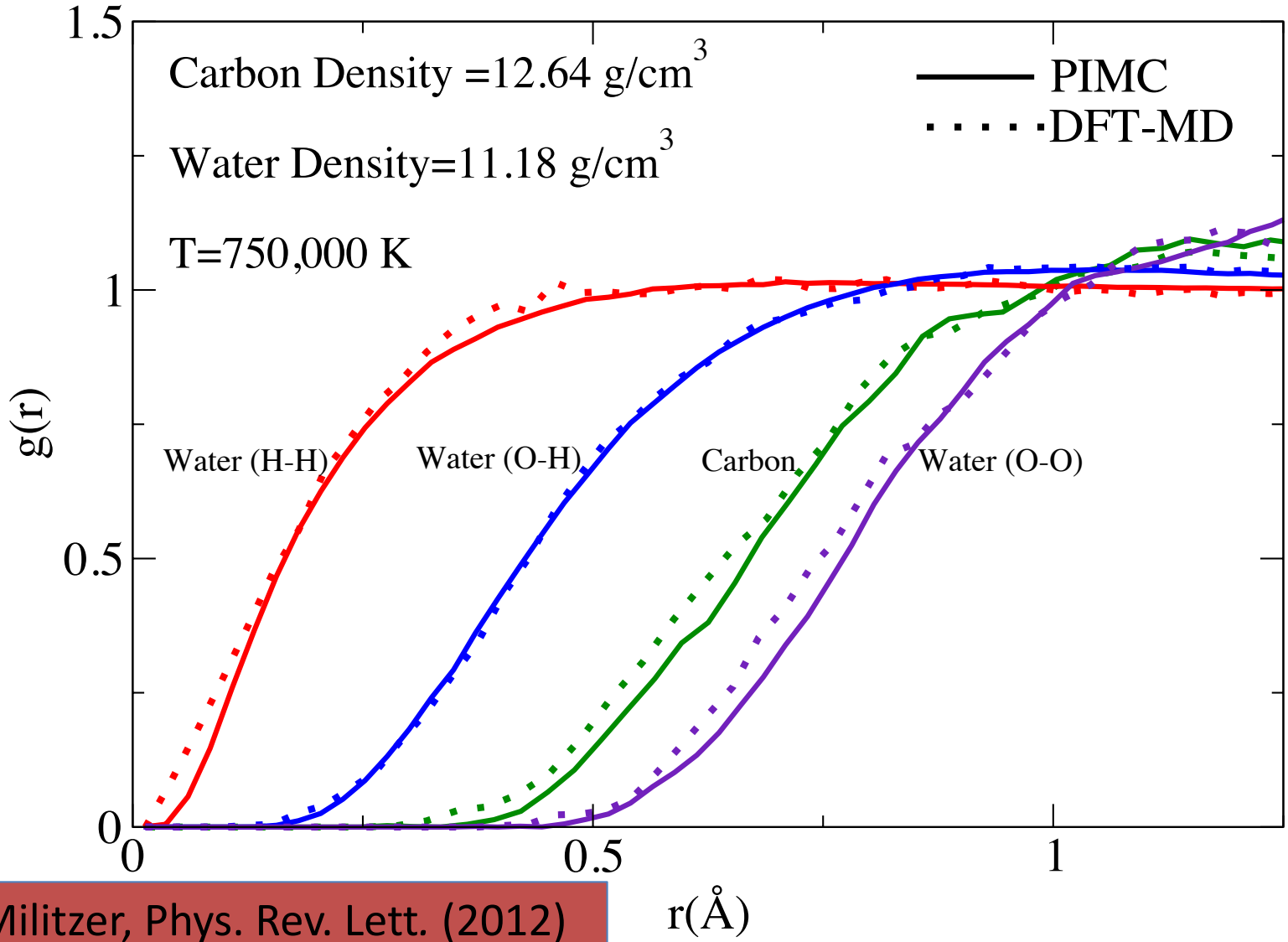

Driver, Militzer, Phys. Rev. Lett. (2012)

Study planetary interiors in the laboratory: shock wave experiments

Two-stage gas gun (Livermore) 0.2 Mbar

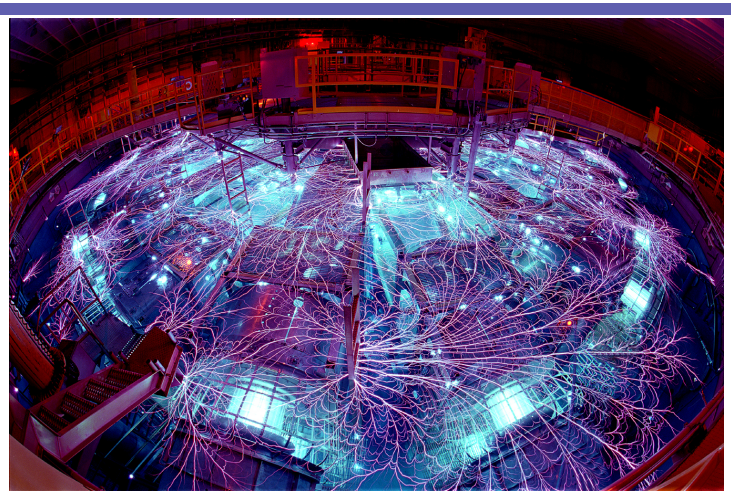

Z capacitor bank (Sandia) 2 Mbar

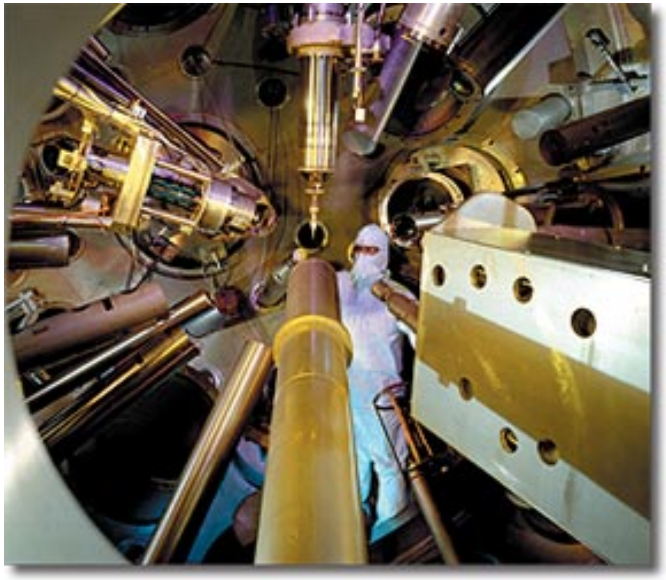

Nova laser (Livermore) 3.4 Mbar

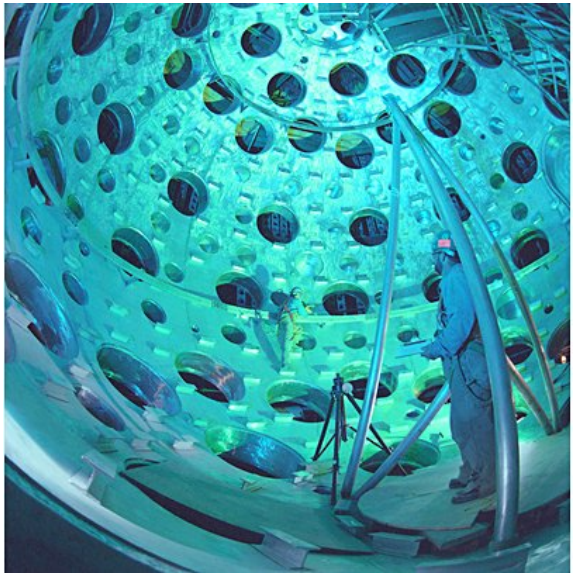

National Ignition Facility 700 Mbar

Shock wave measurements determine the Equation of State on the Hugoniot curve

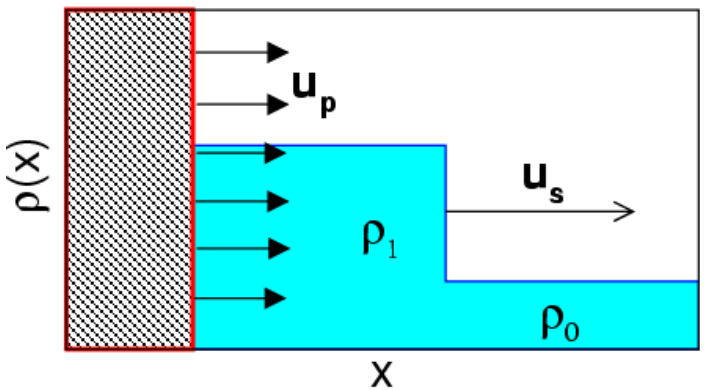

Conservation of mass, momentum and energy yields:

$$\rho = \rho_0 \frac{u_s}{u_s - u_p}$$

$$P = P_0 + \rho_0 u_s u_p$$

$$E = E_0 + \frac{1}{2}(V_0 - V)(P + P_0)$$

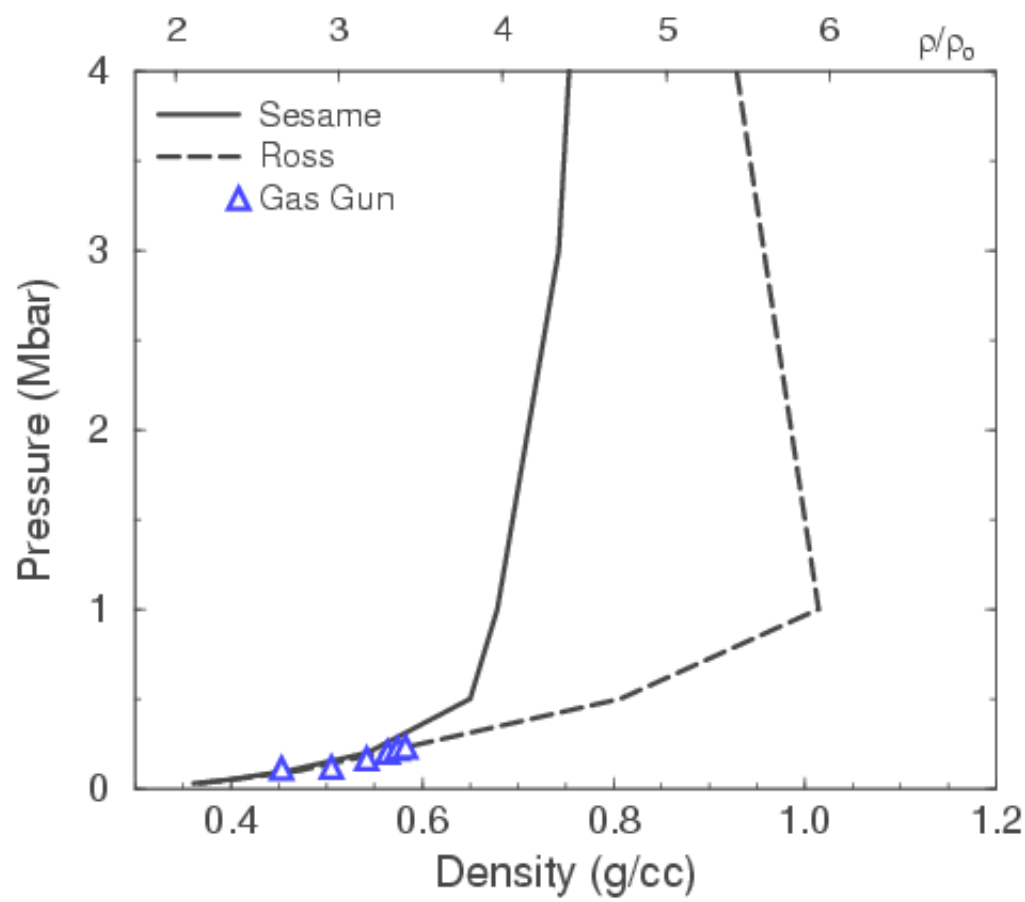

Nitrogen

PIMC and DFT-MD Simulations of Nitrogen

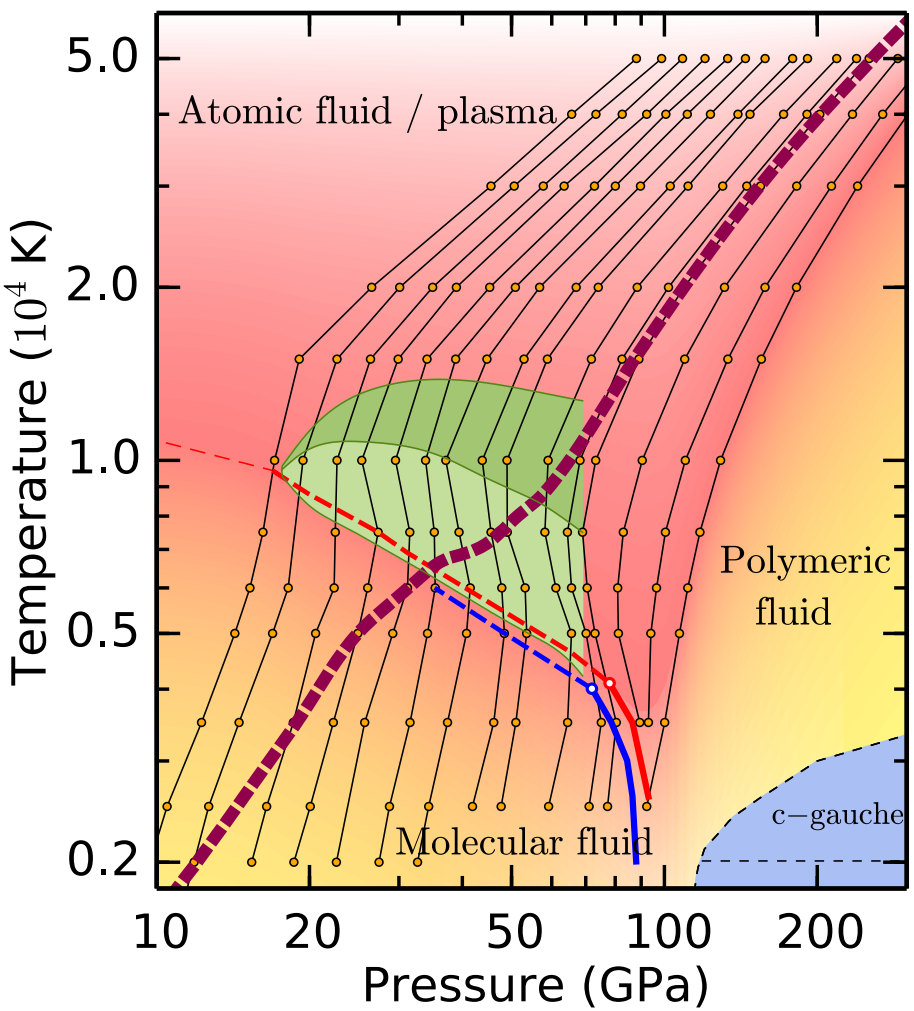

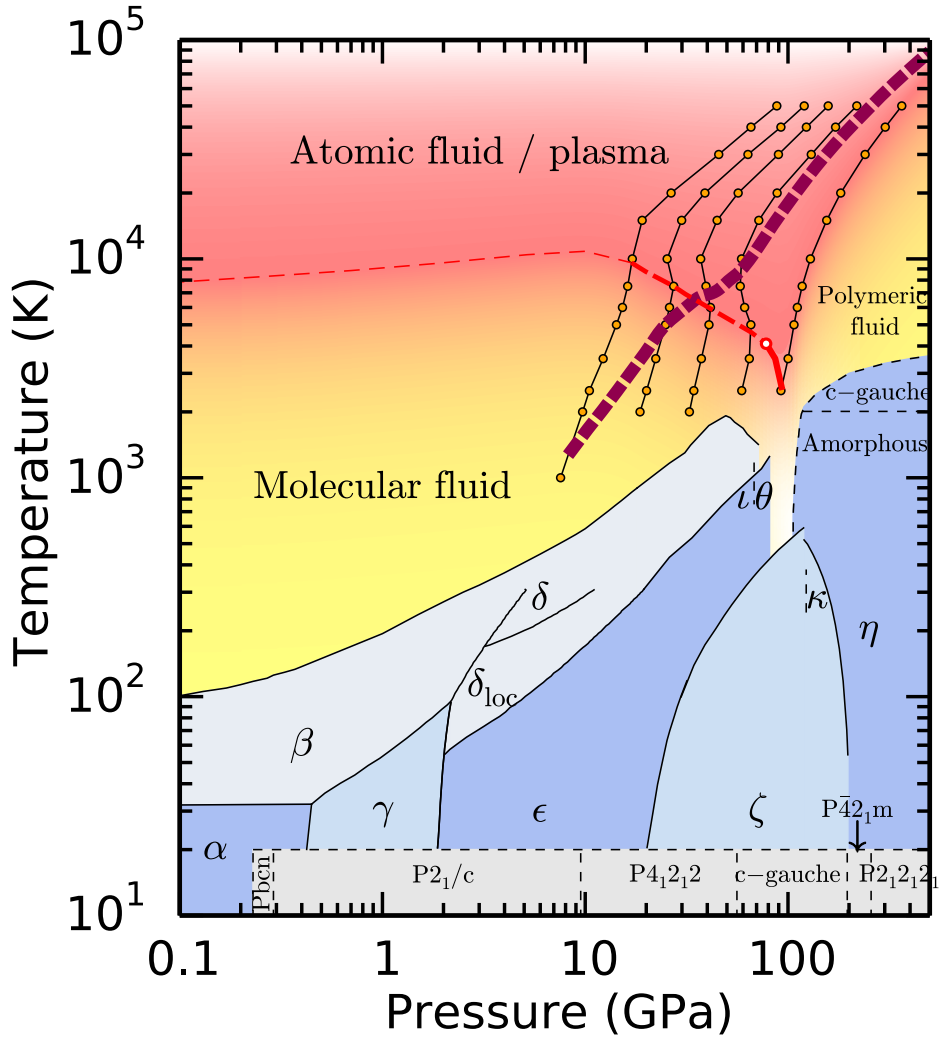

Driver, Militzer, PRB 93, 064101 (2016)

PIMC and DFT-MD Simulations of Nitrogen: How well do pressures and energies agree?

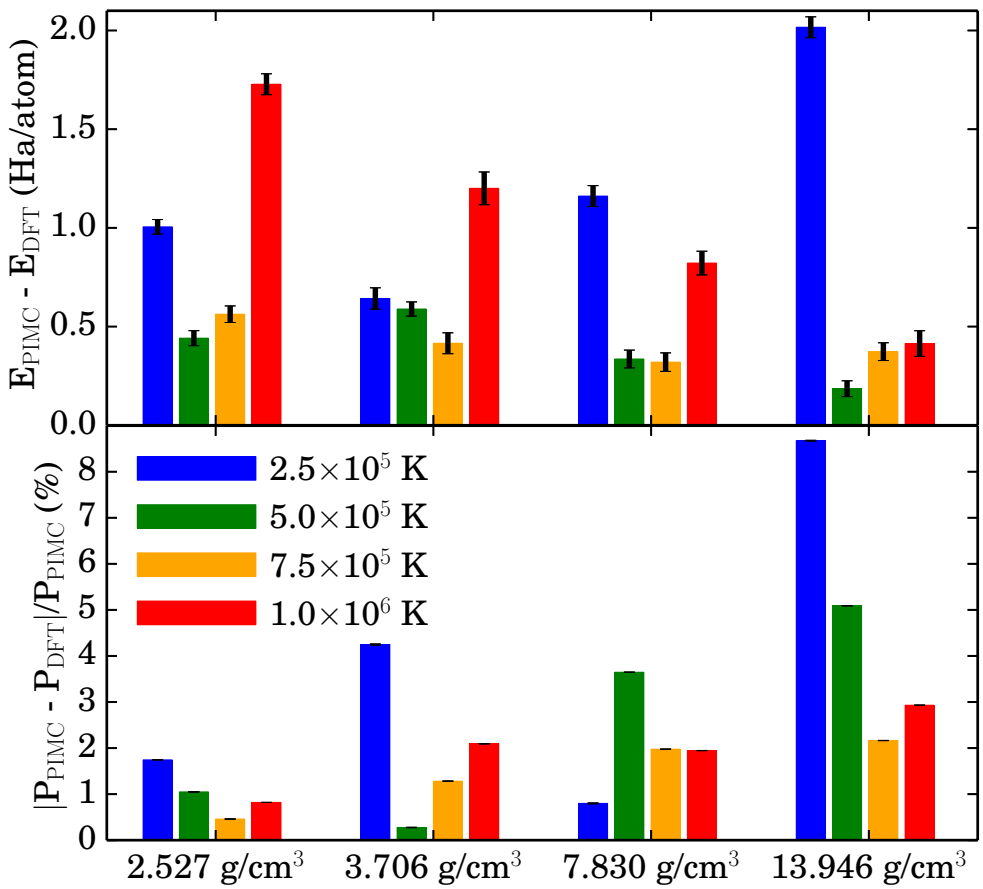

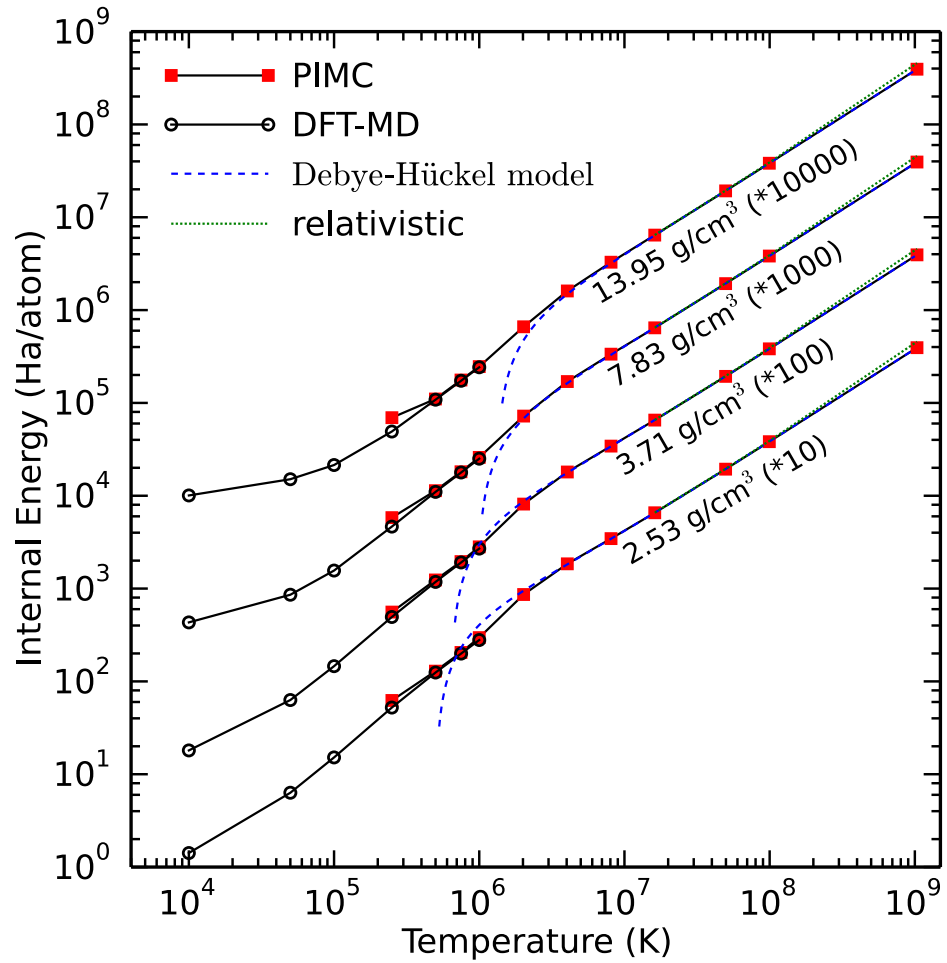

Driver, Militzer, PRB 93, 064101 (2016)

Why do free-particle nodes work for PIMC simulations of first-row elements?

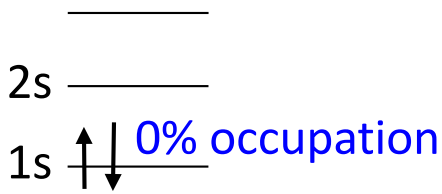

Core electrons are **fully ionized.**
Free-particles nodes are **ideal!**

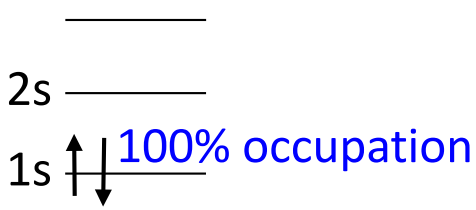

1s state doubly occupied. Others ionized.
Free-particles nodes should still work.

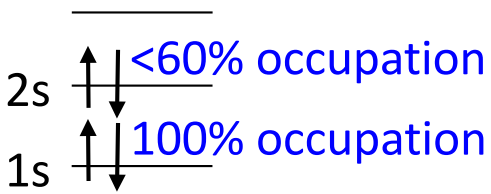

1s 100% occupied, **2s less than 60% occupied**
Free-particles nodes in PIMC are accurate for
T > 250,000 K for carbon and water plasmas.

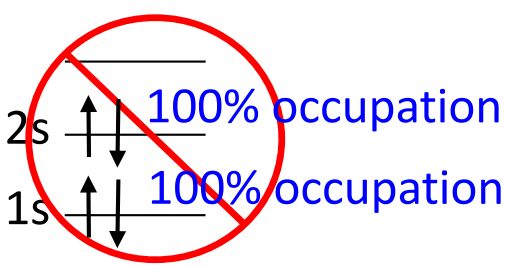

2s 100% occupied. Free-particles nodes do no longer work **but KS-DFT works!**

PIMC and DFT-MD Simulations of Nitrogen: Comparison with Experiments and Theory

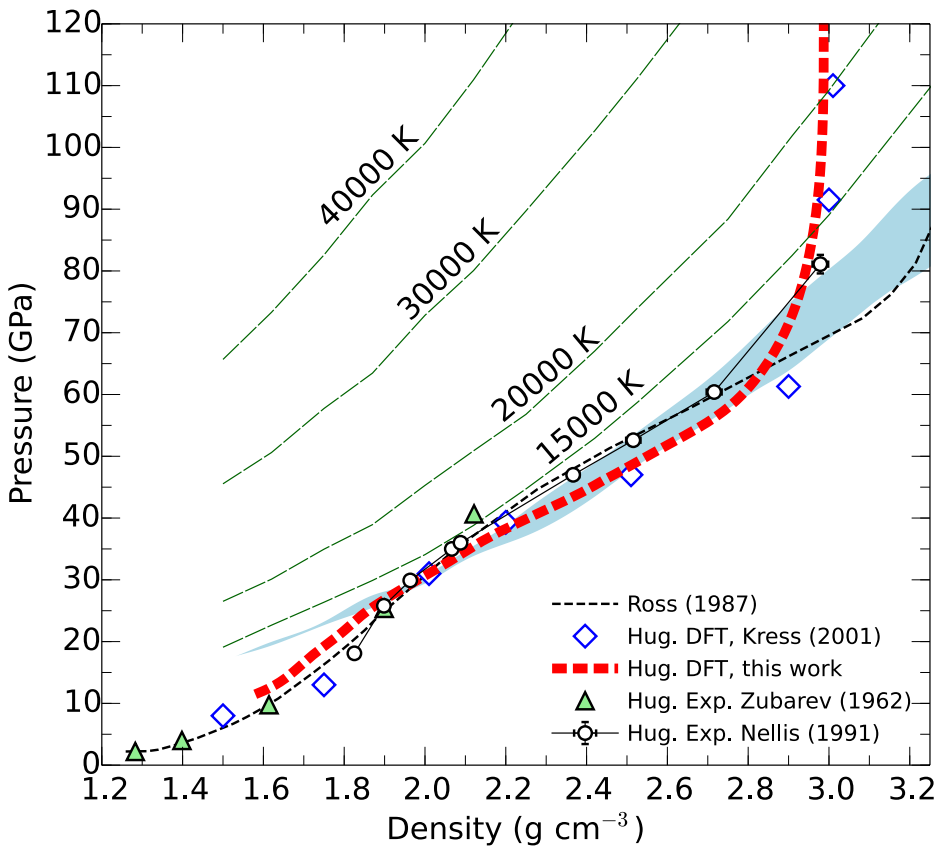

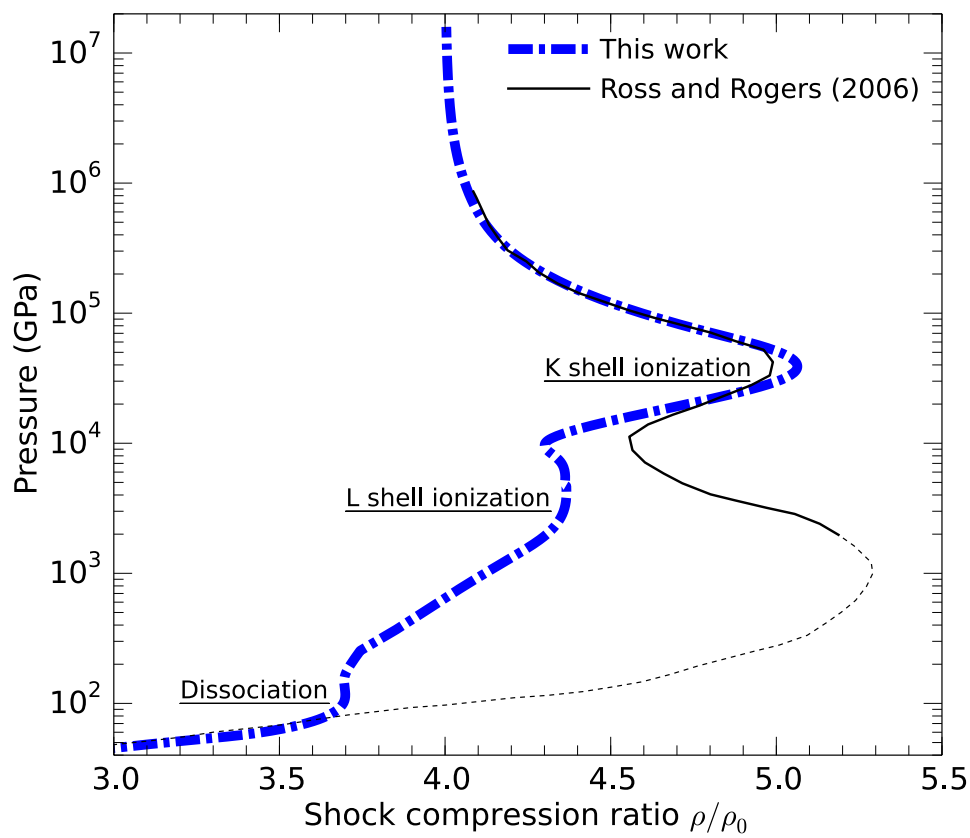

Driver, Militzer, PRB 93, 064101 (2016)

PIMC and DFT-MD Simulations of Nitrogen: Poor Agreement with Experiments by Mochalov (2010)

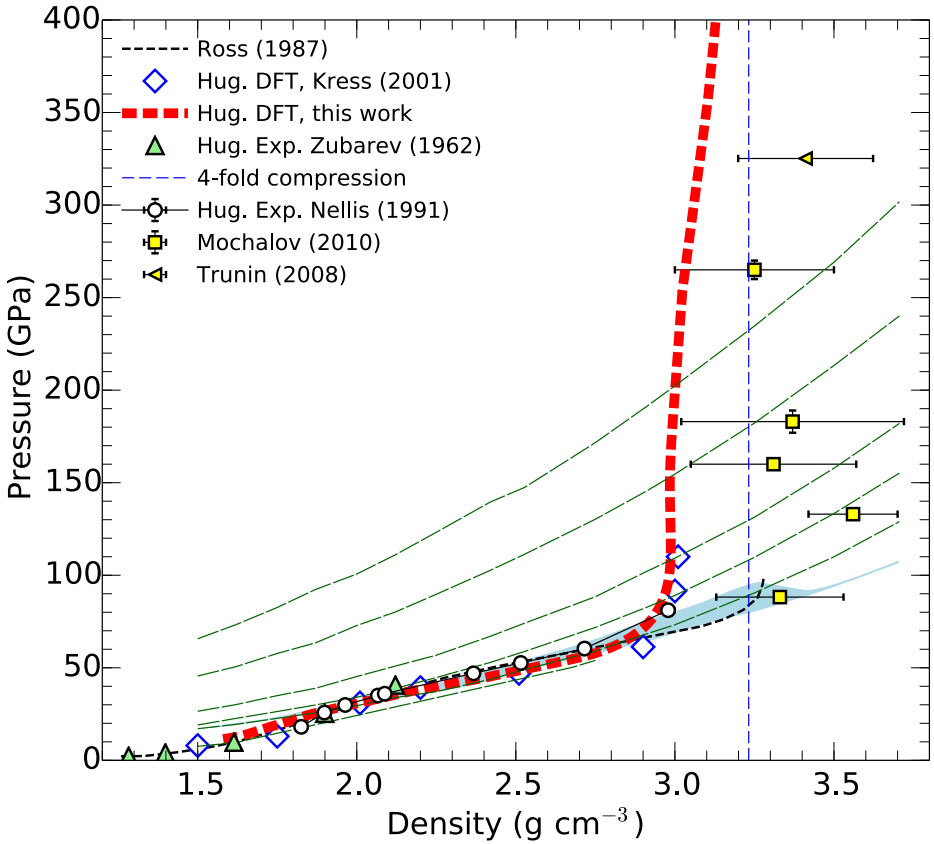

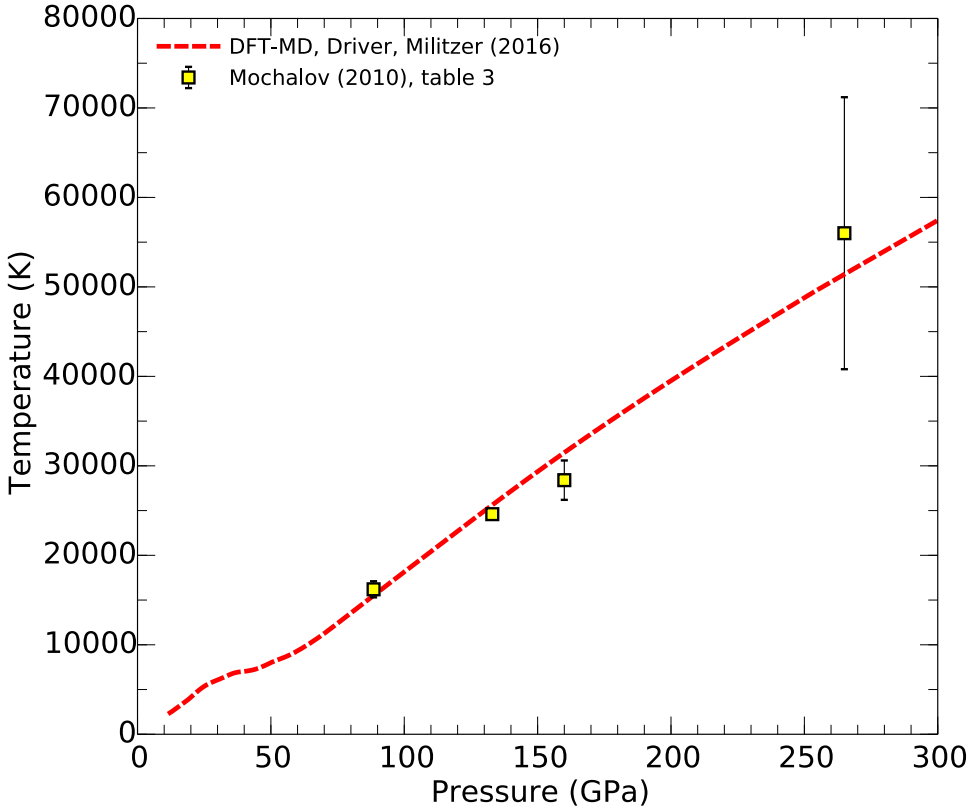

Driver, Militzer, PRB 93, 064101 (2016)

CH plastics

Inertial confinement fusion experiments with plastic coated spheres of liquid H_2

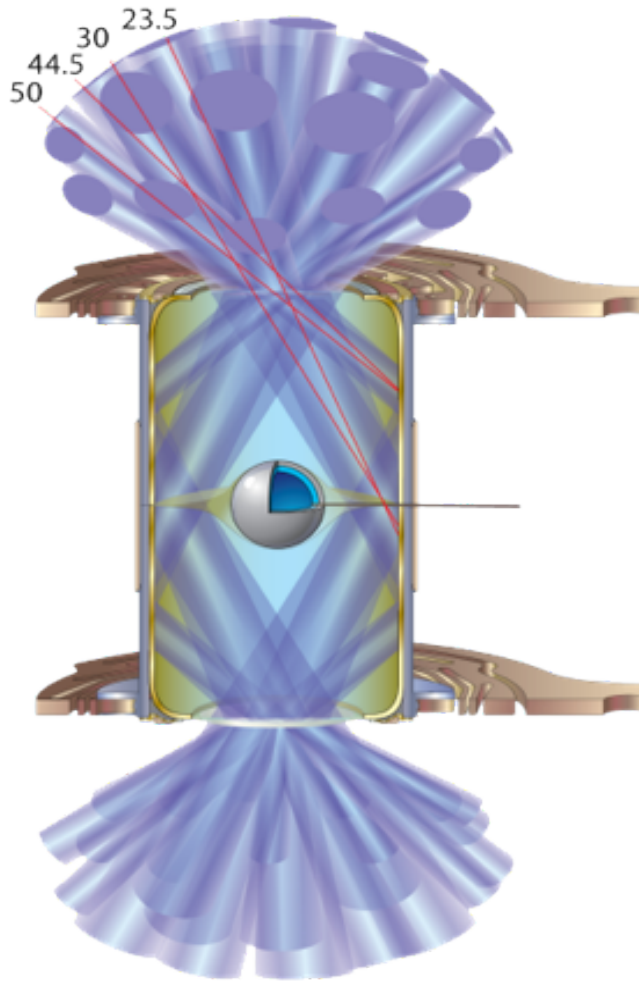

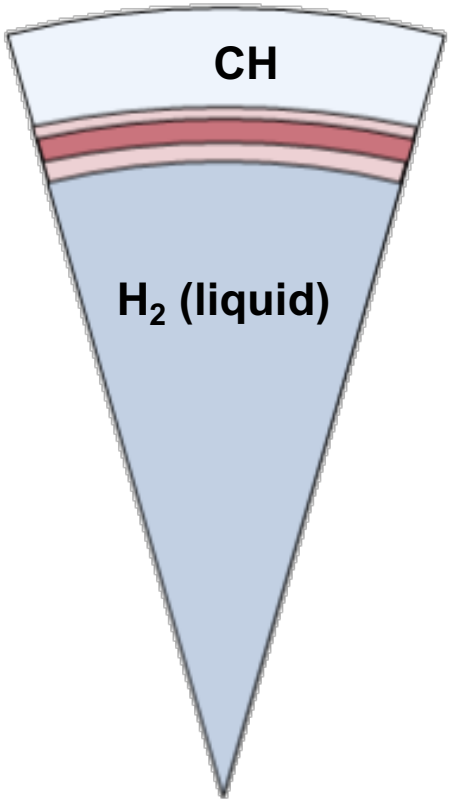

(Graphics: Bachmann et al. LLNL)

PIMC and DFT-MD simulations performed for C_2H, CH, C_2H_3, CH_3 and CH_4.

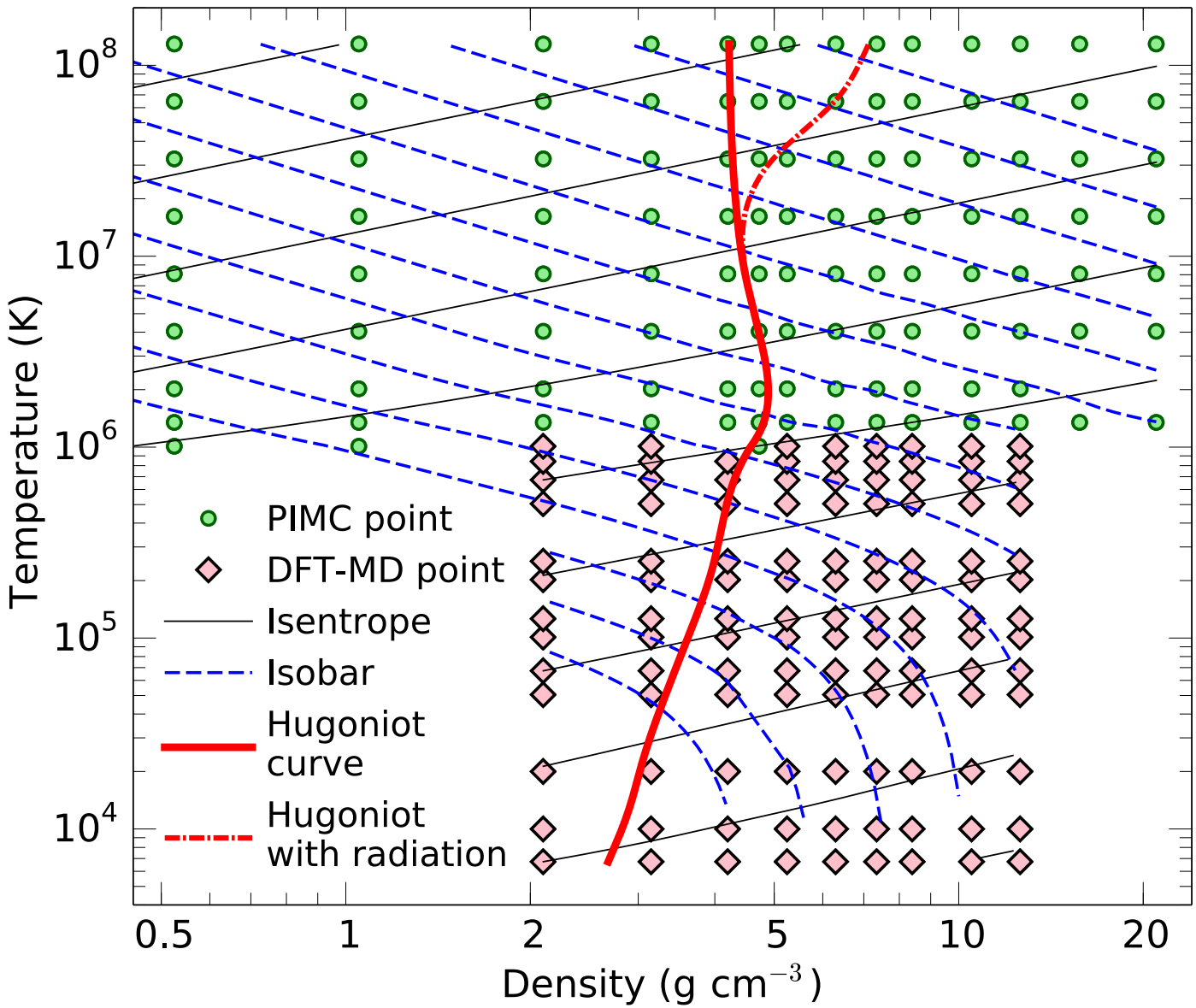

CH Shock Hugoniot Curves: Comparison of Theory and Experiments

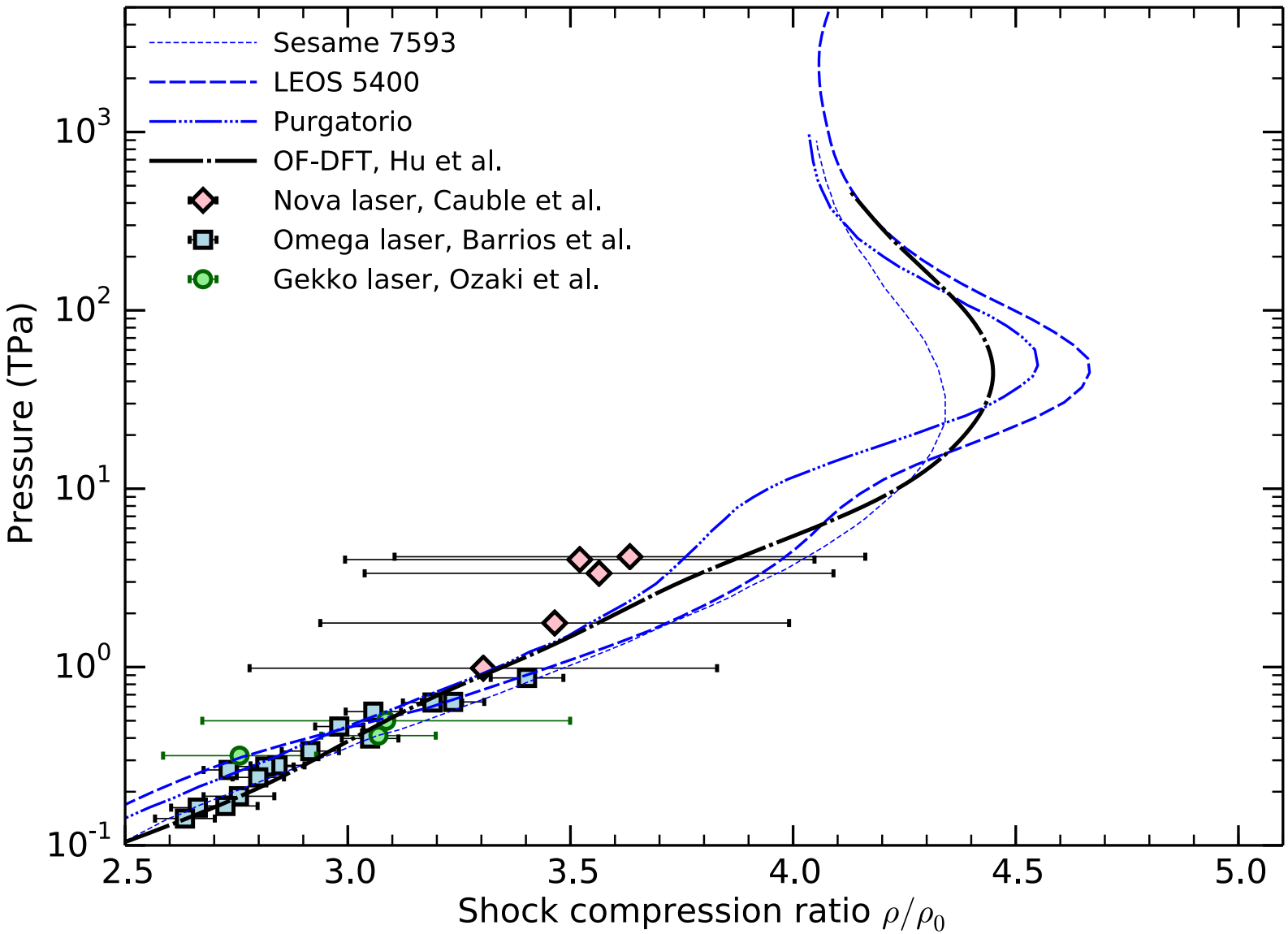

CH Shock Hugoniot Curves: Comparison of Theory and Experiments

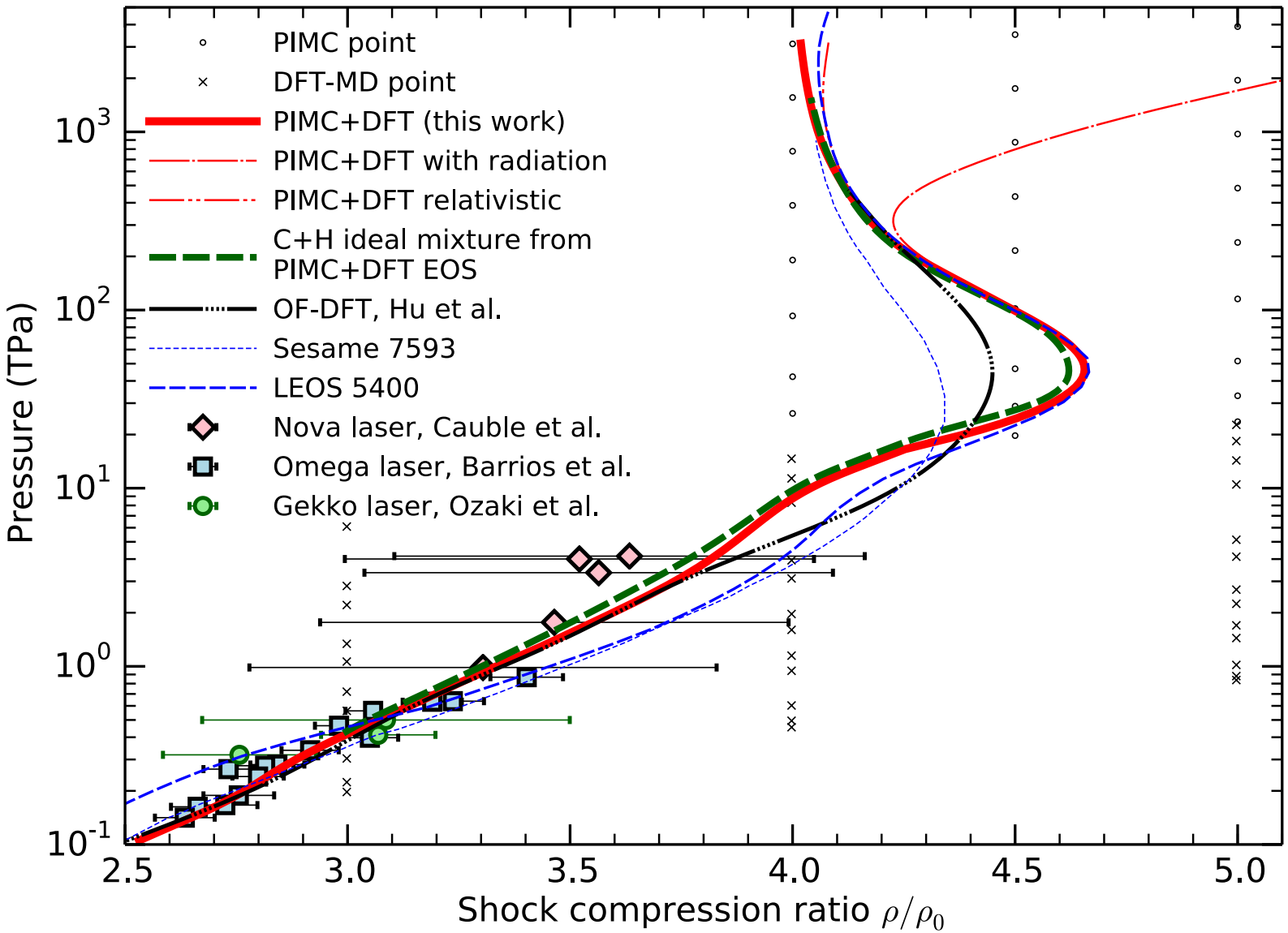

Linear Mixing Approximation works well

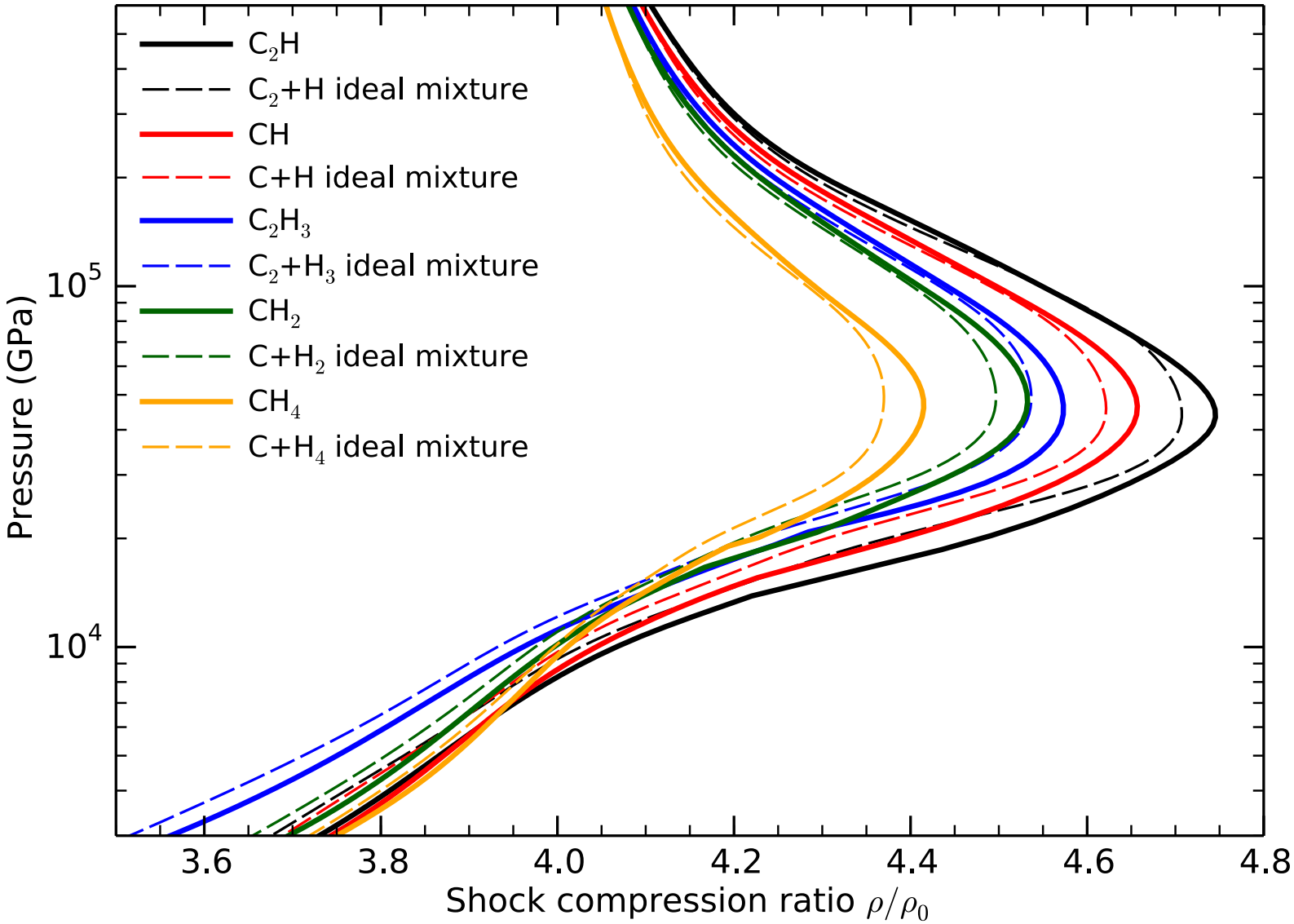

Why do the C and CH Hugoniot curves differ from those for N, O and Ne?

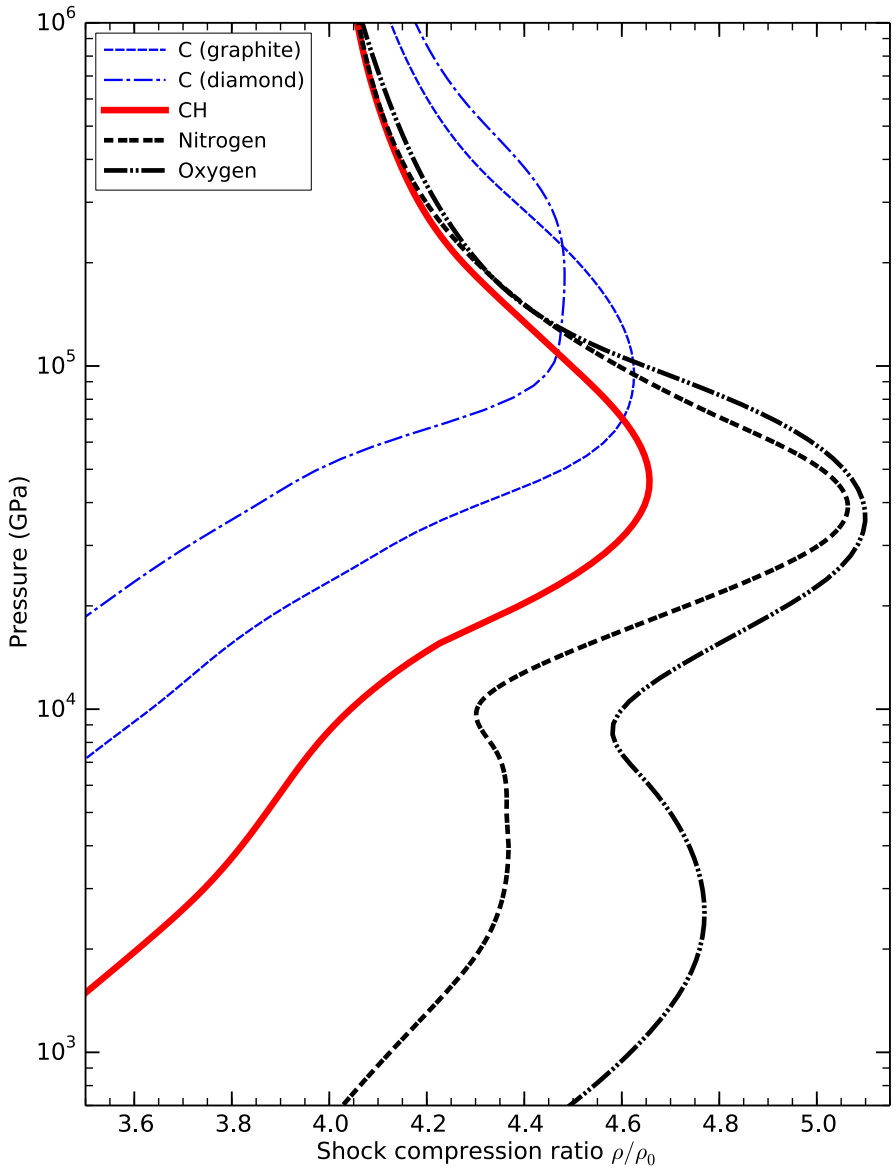

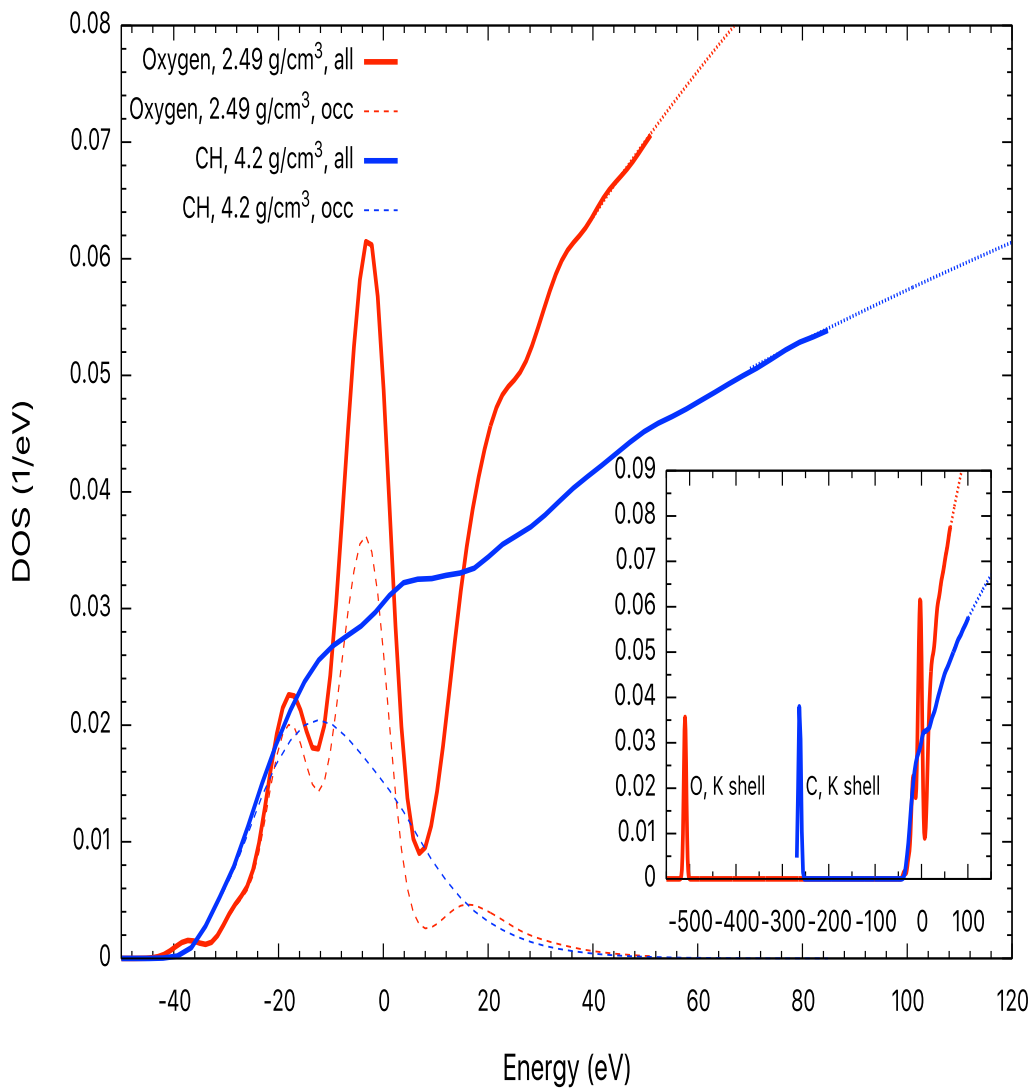

Phys. Rev. E, in press, arXiv:1706.09073

Silicon

Path Integral Monte Carlo with localized nodal surfaces and application to silicon plasmas

How the nodes are enforced:

$$\rho_F(\mathbf{R},\mathbf{R}';\beta) = \frac{1}{N!}\sum_{\mathcal{P}}(-1)^{\mathcal{P}}\int_{\mathbf{R}\to\mathcal{P}\mathbf{R}',\,\rho_T>0} \mathbf{dR}_t\;\; e^{-S[\mathbf{R}_t]}$$

Nodes are a Slater determinant:

$$\rho_T(\mathbf{R},\mathbf{R}';\beta) = \left|\left|\rho^{[1]}(r_i,r'_j;\beta)\right|\right|_{ij}$$

Before we used only free-particle orbitals (plane waves):

$$\rho_0^{[1]}(r,r';\beta) = \sum_k e^{-\beta E_k}\,\Psi_k(r)\,\Psi_k^*(r')$$

New idea: Add Hartree-Fock orbitals

$$\rho^{[1]}(r,r',\beta) = \sum_{I=1}^{N}\sum_{s=0}^{n} e^{-\beta E_s}\Psi_s(r-R_I)\Psi_s^*(r'-R_I)$$

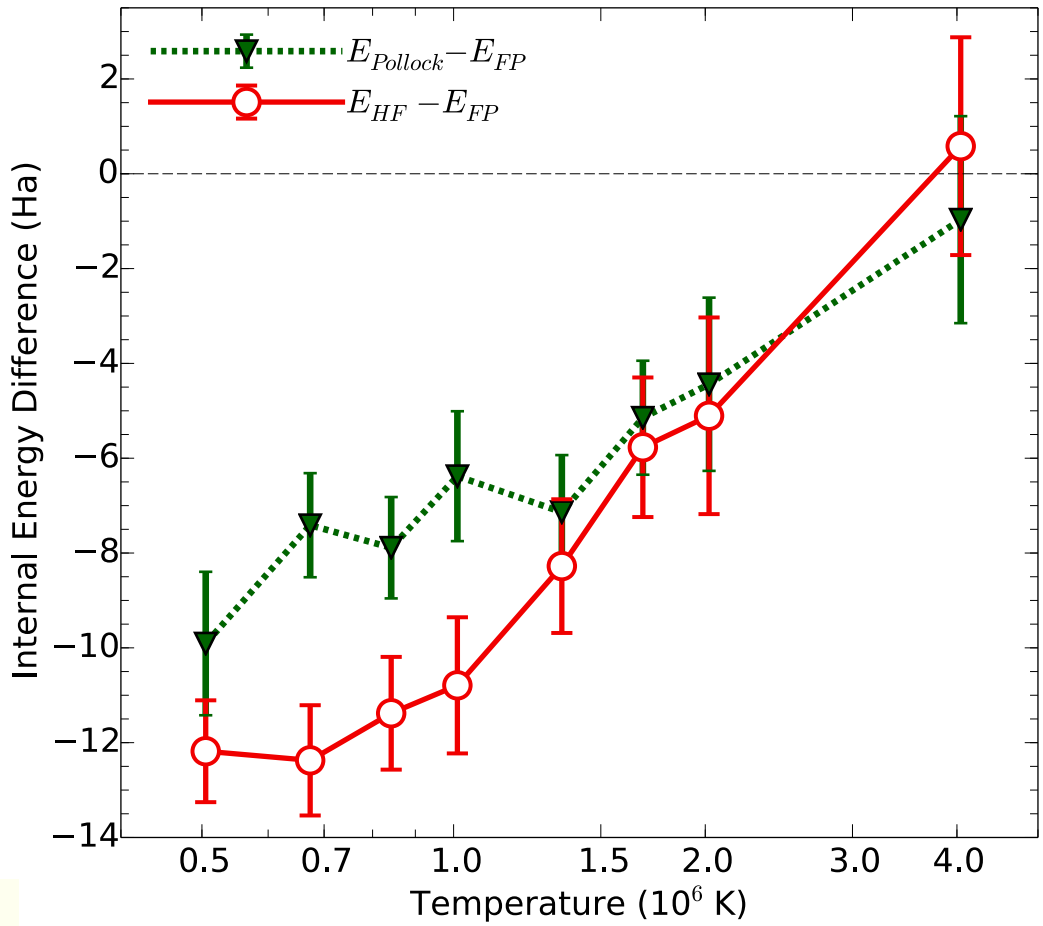

Militzer, Driver, Phys. Rev. Lett. (2015)

New Type of PIMC Move needed: Multi-Particle Moves

- Since the nodes depend on the nuclei, need to move ions and nearby electrons at once.
- Which electrons are nearby? Use localization function:

$$L_{Ij} = \int_0^\beta dt\ |\Psi_{1s}(r_j(t) - R_I)|^2$$

- Build a table of ion-electron moves with up to 4 electrons.
- Sample from it like the permutation table.
- This led to efficient PIMC simulations.

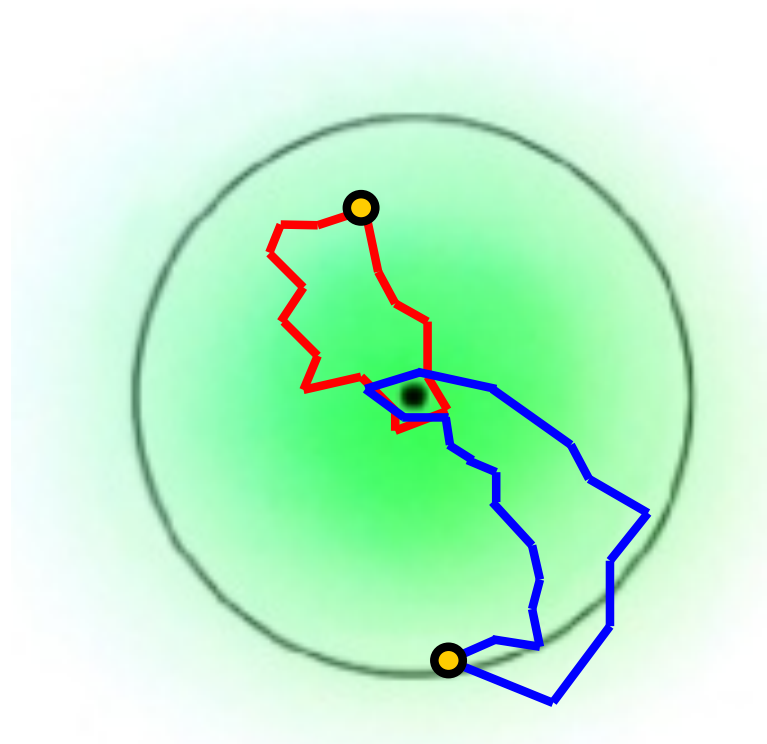

Militzer, Driver, Phys. Rev. Lett. (2015)

Energy and Pressure Comparison of Path Integral Monte Carlo and Kohn-Sham DFT

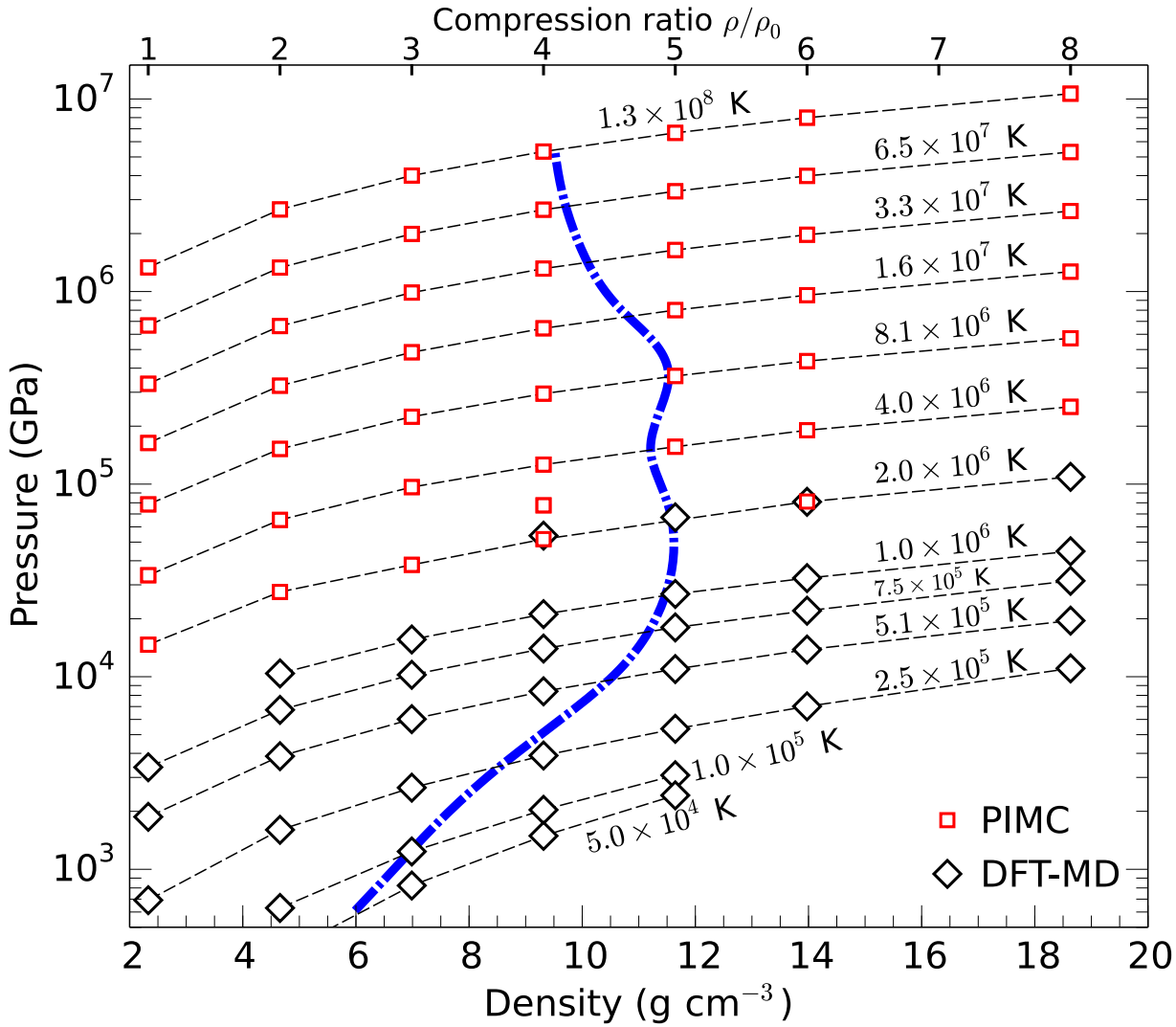

Militzer, Driver, Phys. Rev. Lett. (2015)

Silicon: Energy and Pressure Comparison of Path Integral Monte Carlo and Kohn-Sham DFT

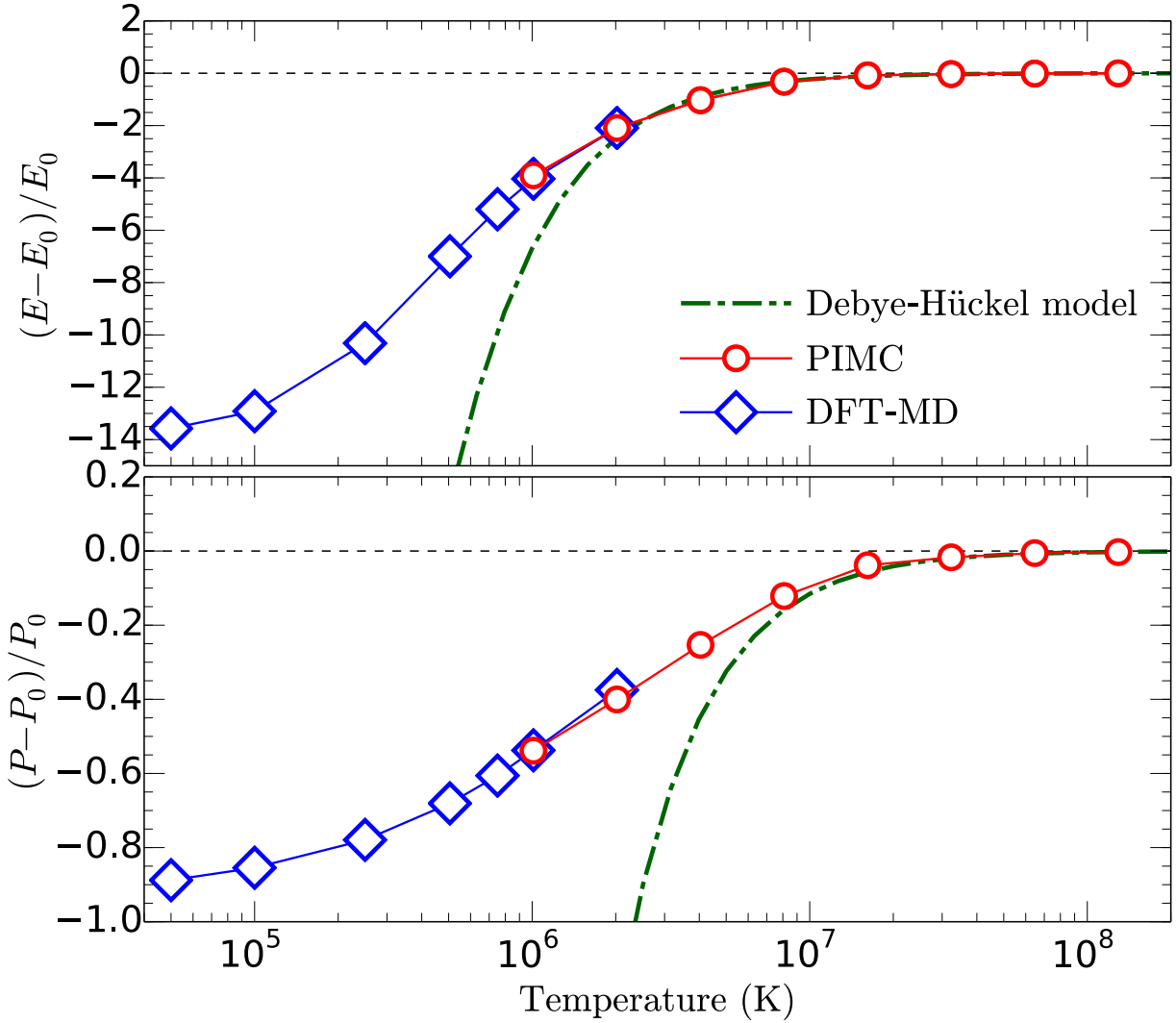

Militzer, Driver, Phys. Rev. Lett. (2015)

Energy of isolated silicon atom: Path Integral Monte Carlo and Orbital-Free DFT

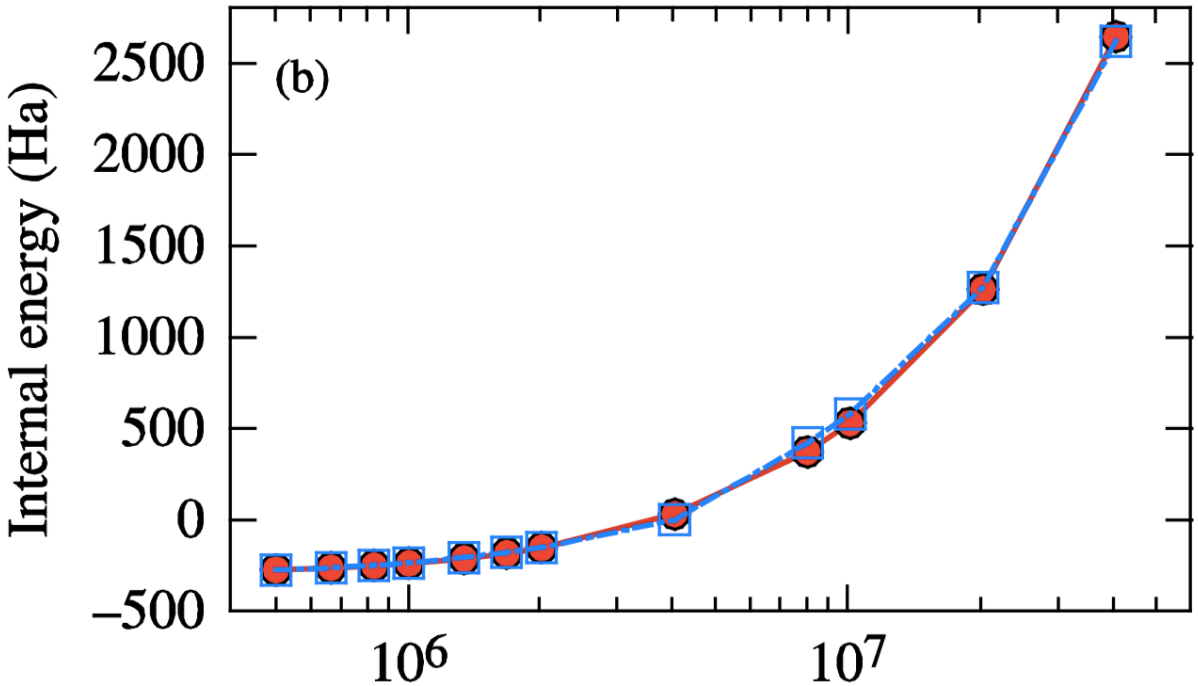

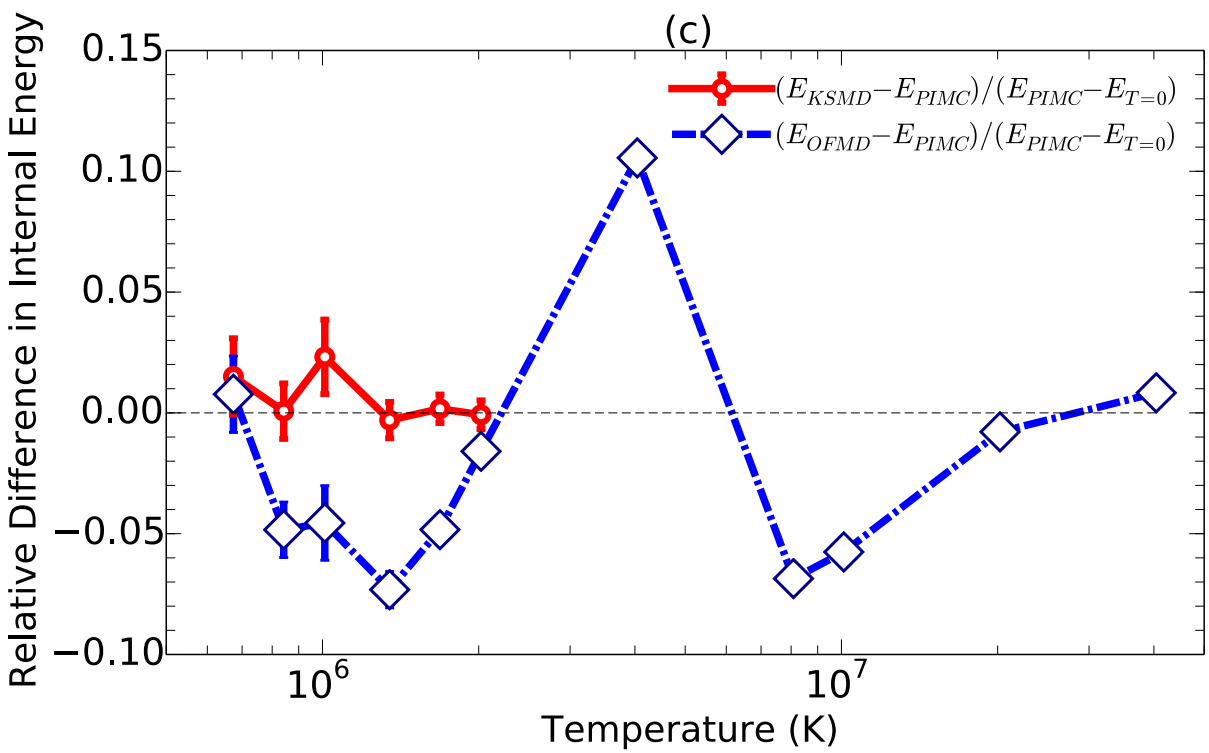

Hu, Militzer, Collins, Driver, Kress, Phys. Rev. B 94 (2016) 094109

g(r) Comparison of Path Integral Monte Carlo and Kohn-Sham DFT

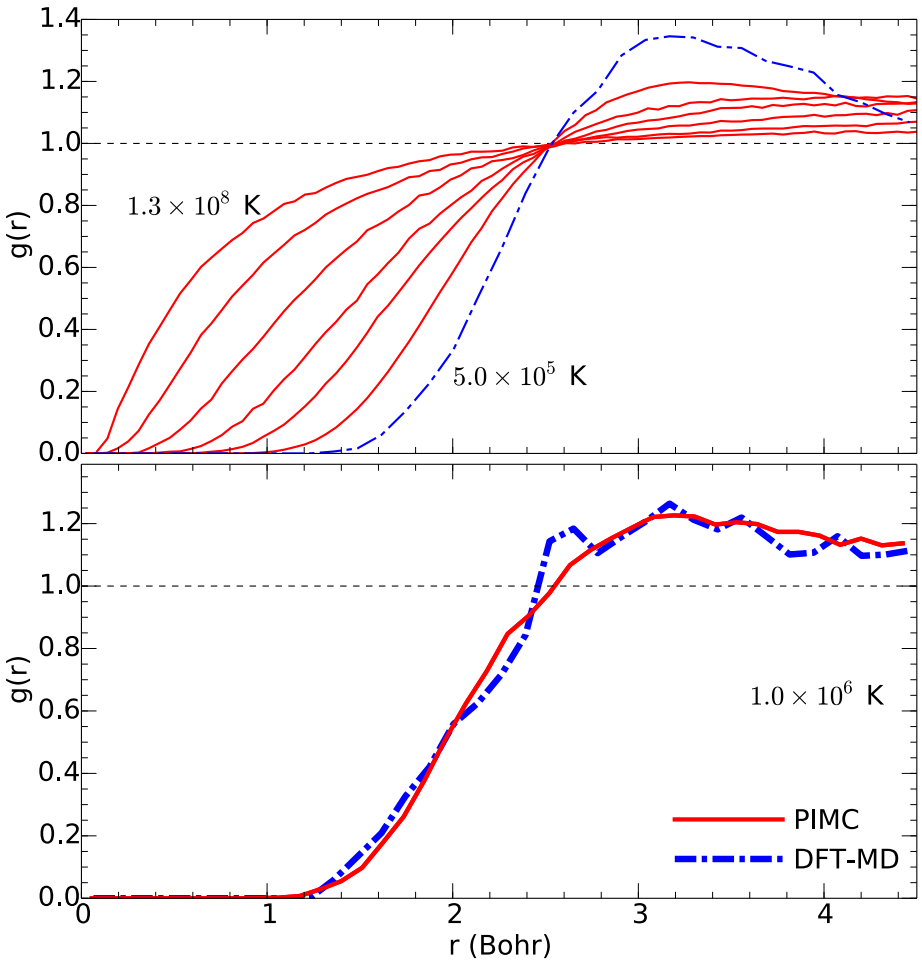

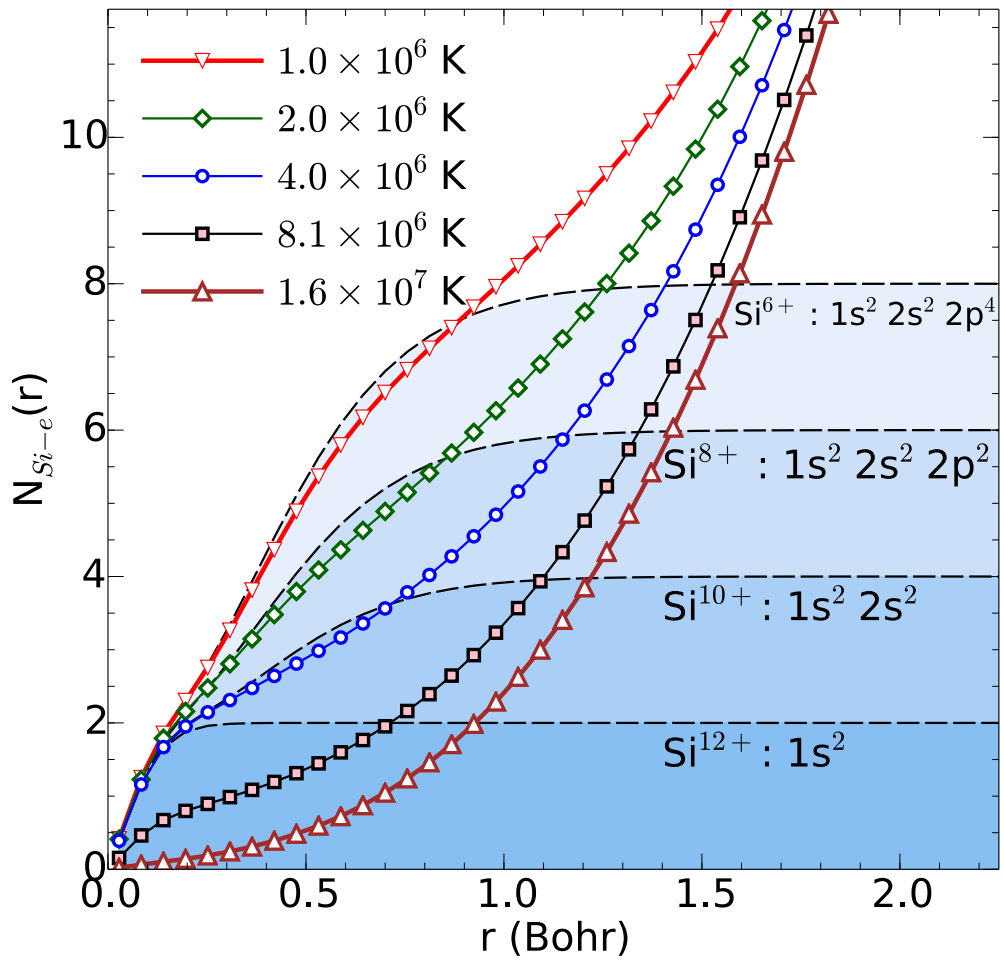

Militzer, Driver, Phys. Rev. Lett. (2015)

Energy and Pressure Comparison of Path Integral Monte Carlo & Orbital-Free DFT

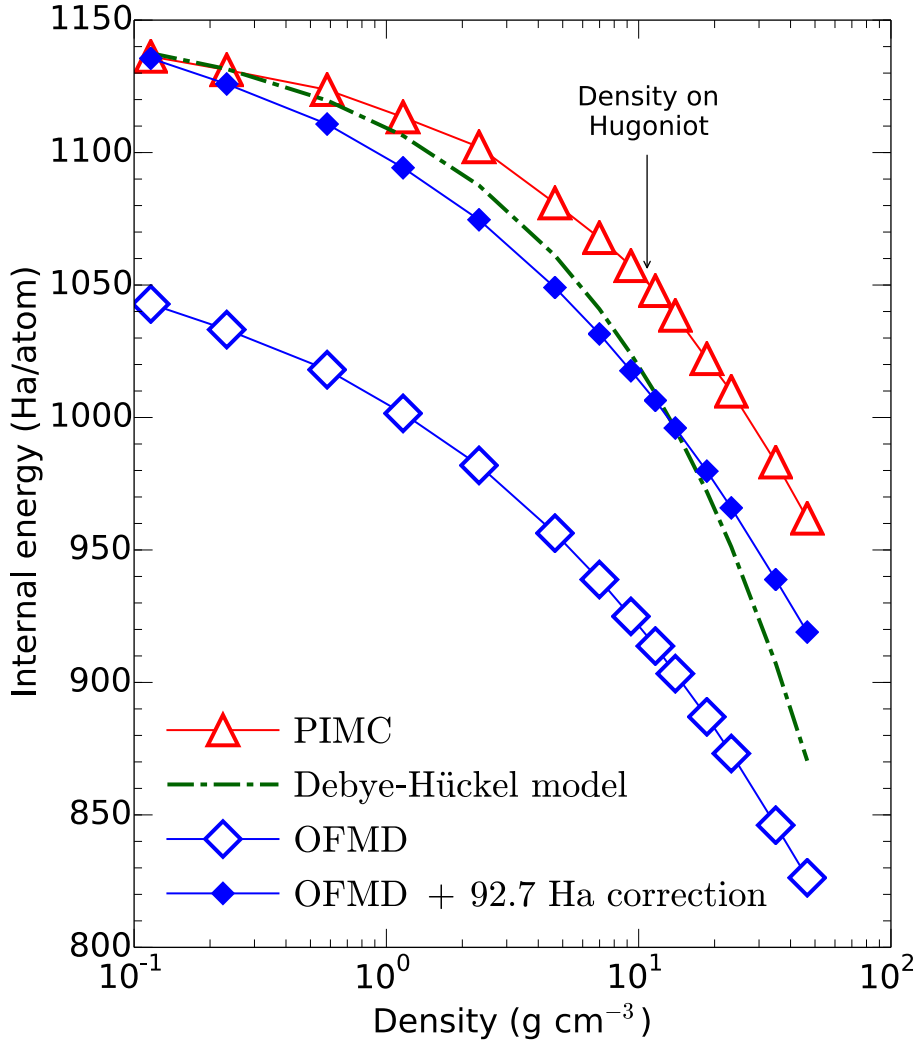

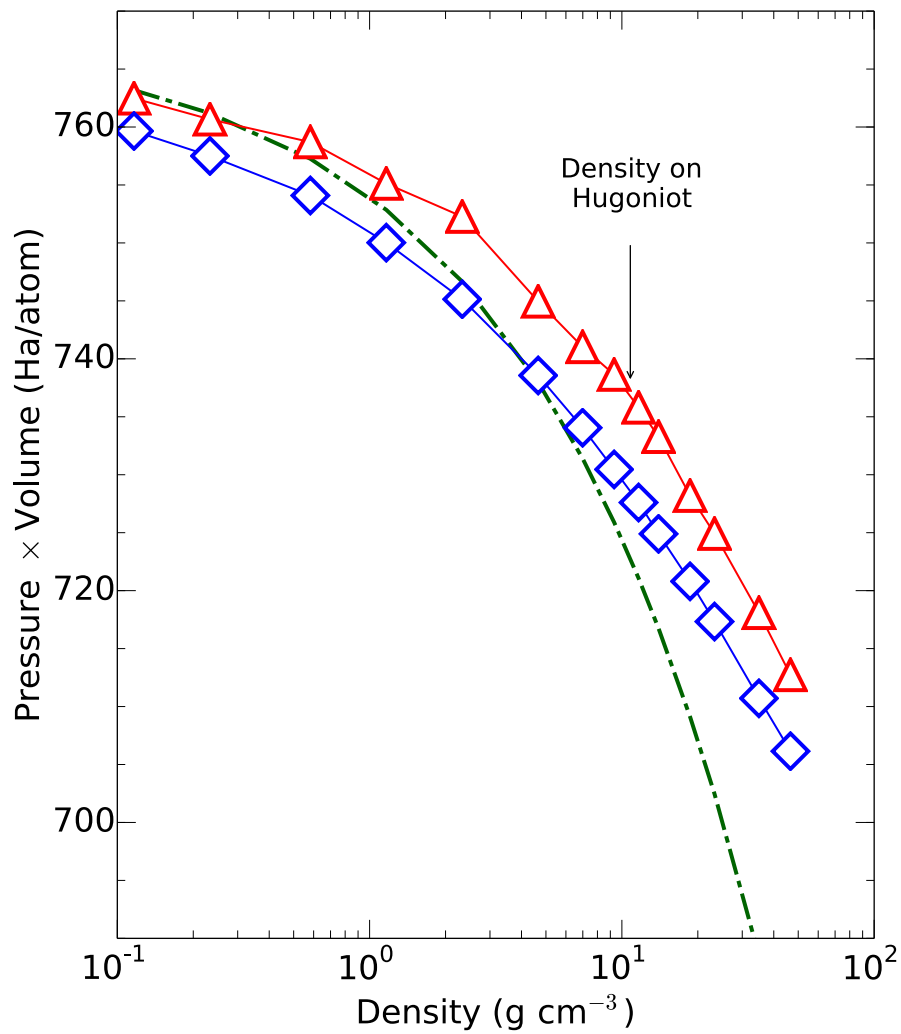

Hu, Militzer, Collins, Driver, Kress, Phys. Rev. B 94 (2016) 094109

Silicon Hugoniot Curve:
Experiments and Semi-analytical EOS models

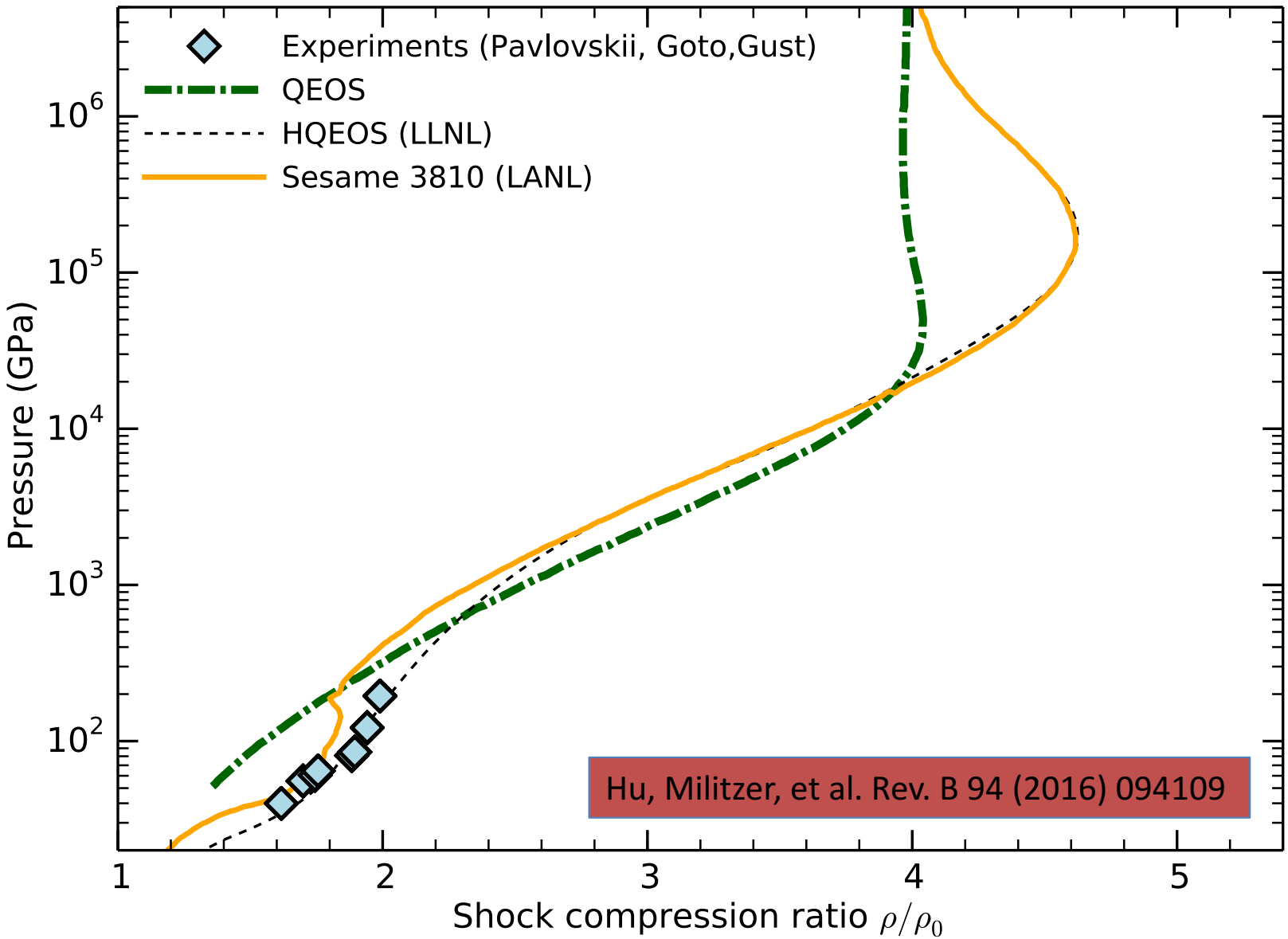

Silicon Hugoniot Curve:
Path Integral Monte Carlo, Orbital-Free DFT

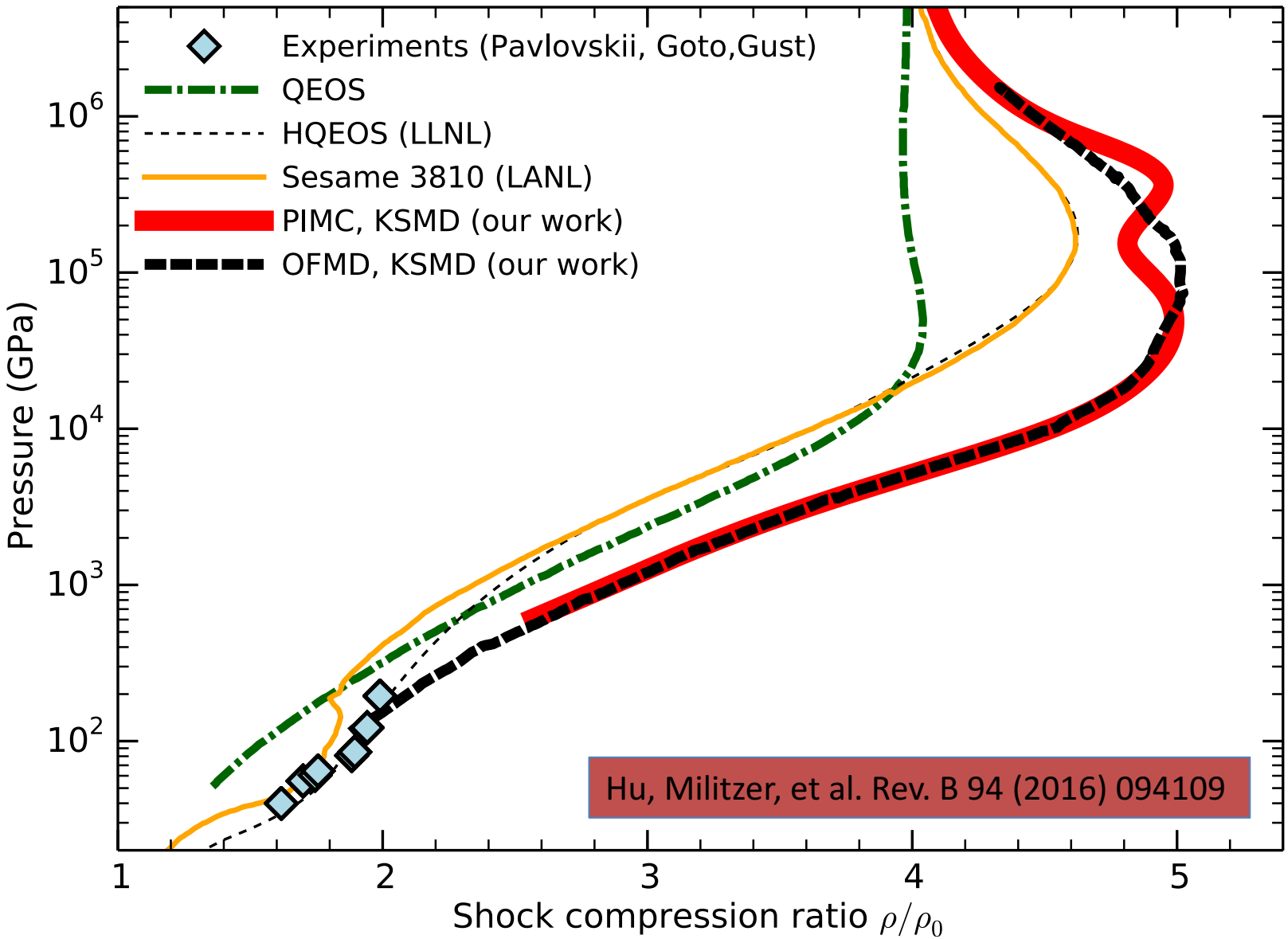

Silicon Hugoniot Curve:
Average-Atom models

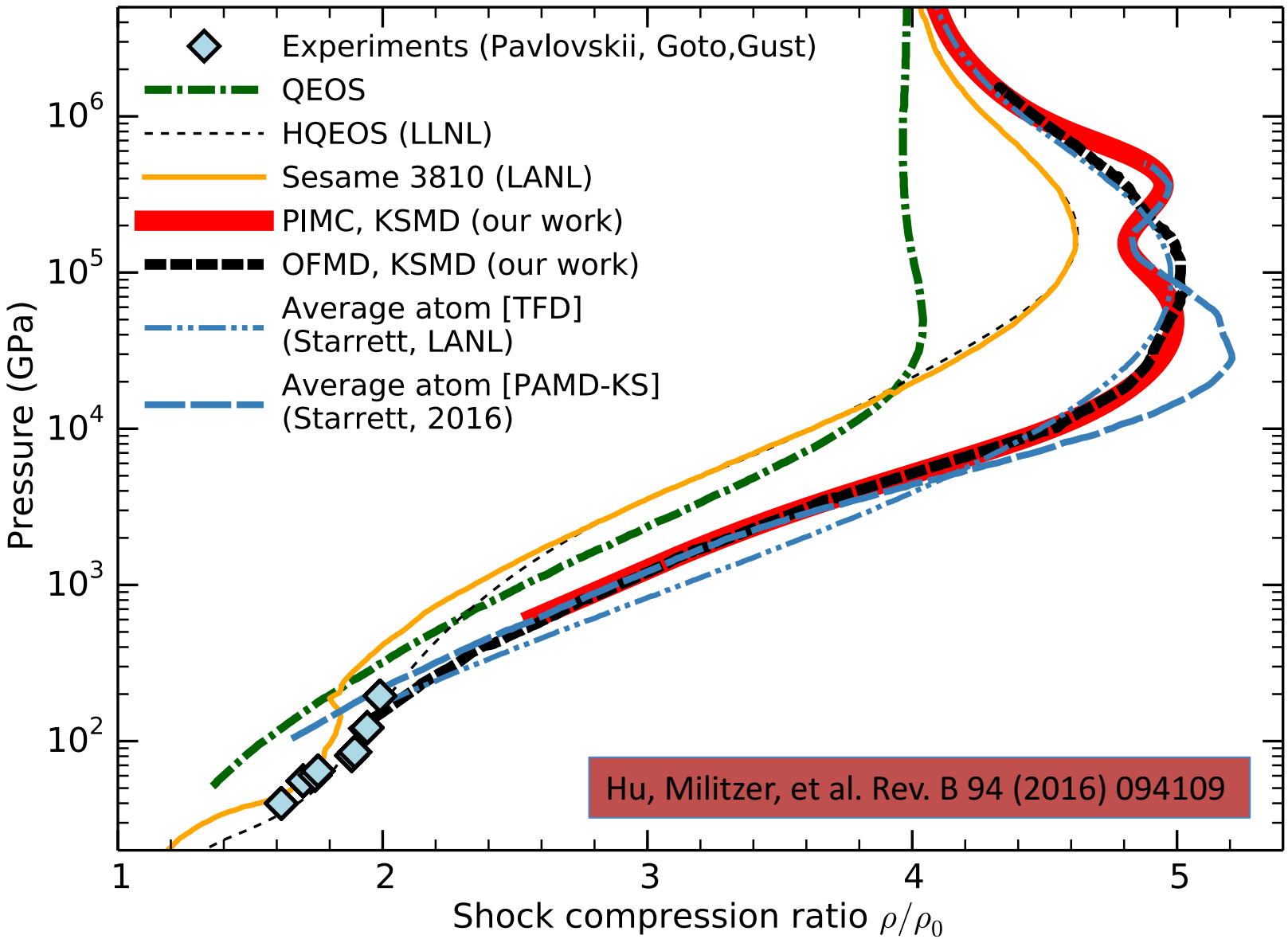

Comparison of Hugoniot Curves for Different Materials

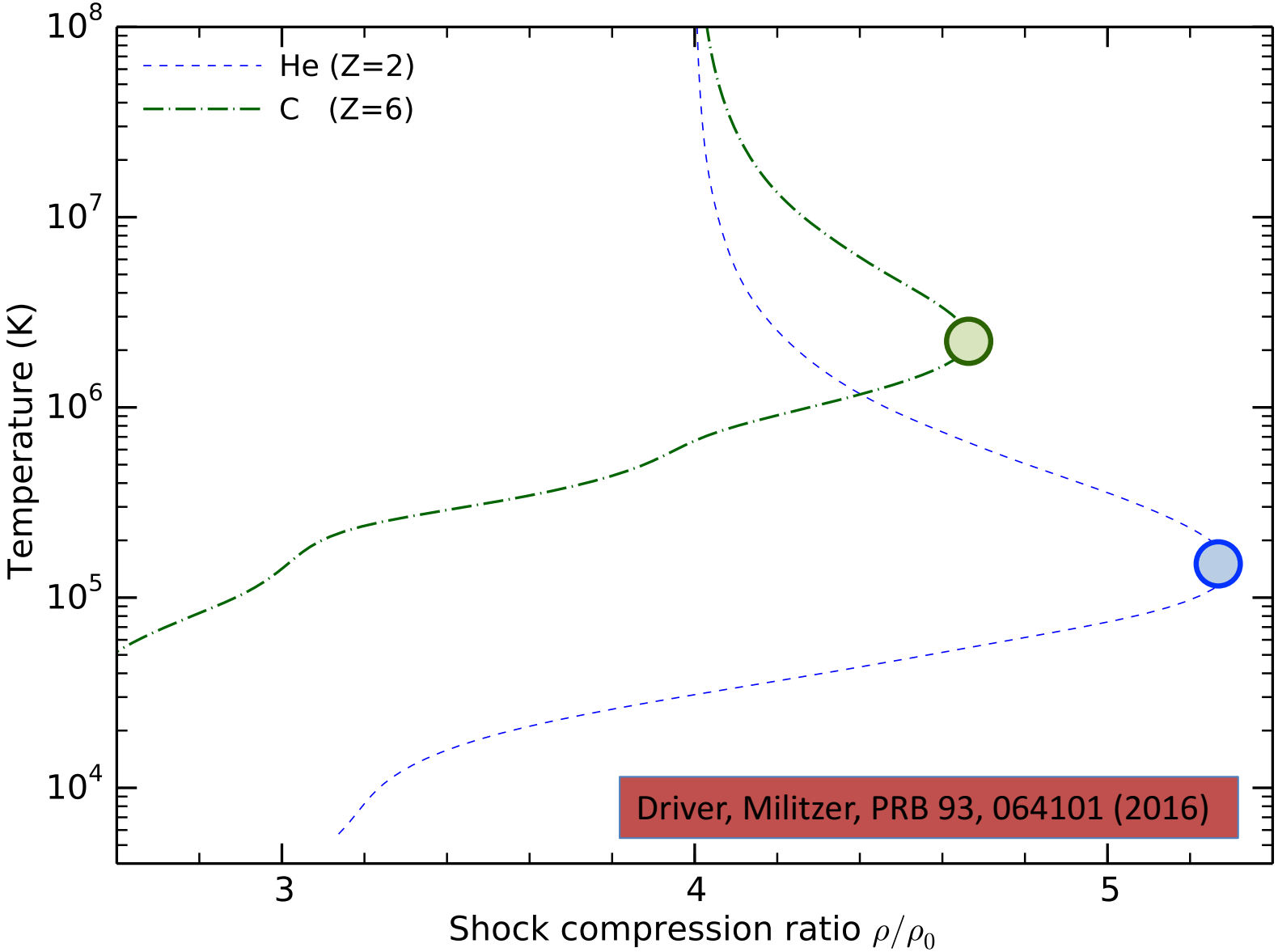

Comparison of Hugoniot Curves for Different Materials

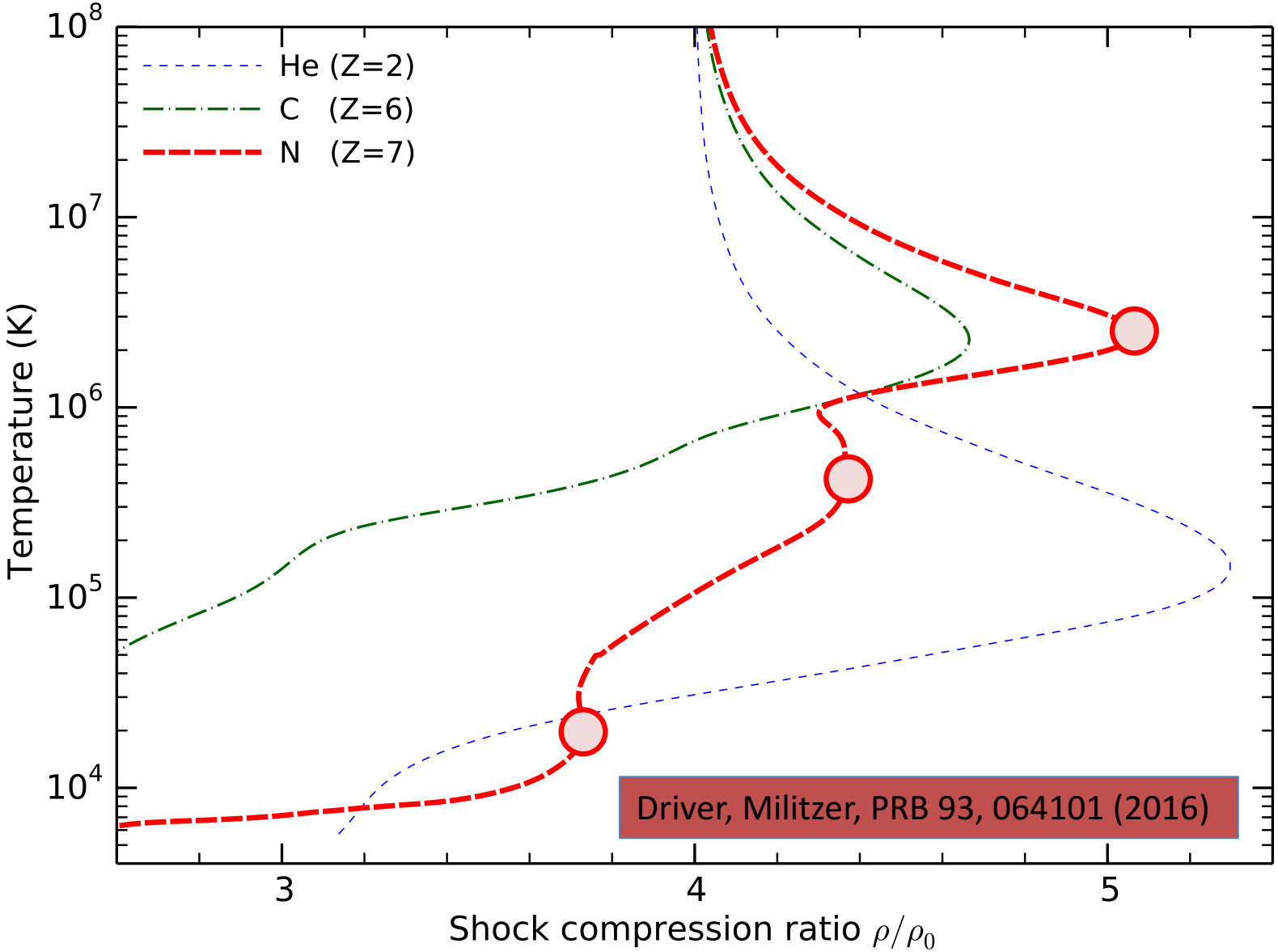

Comparison of Hugoniot Curves for Different Materials

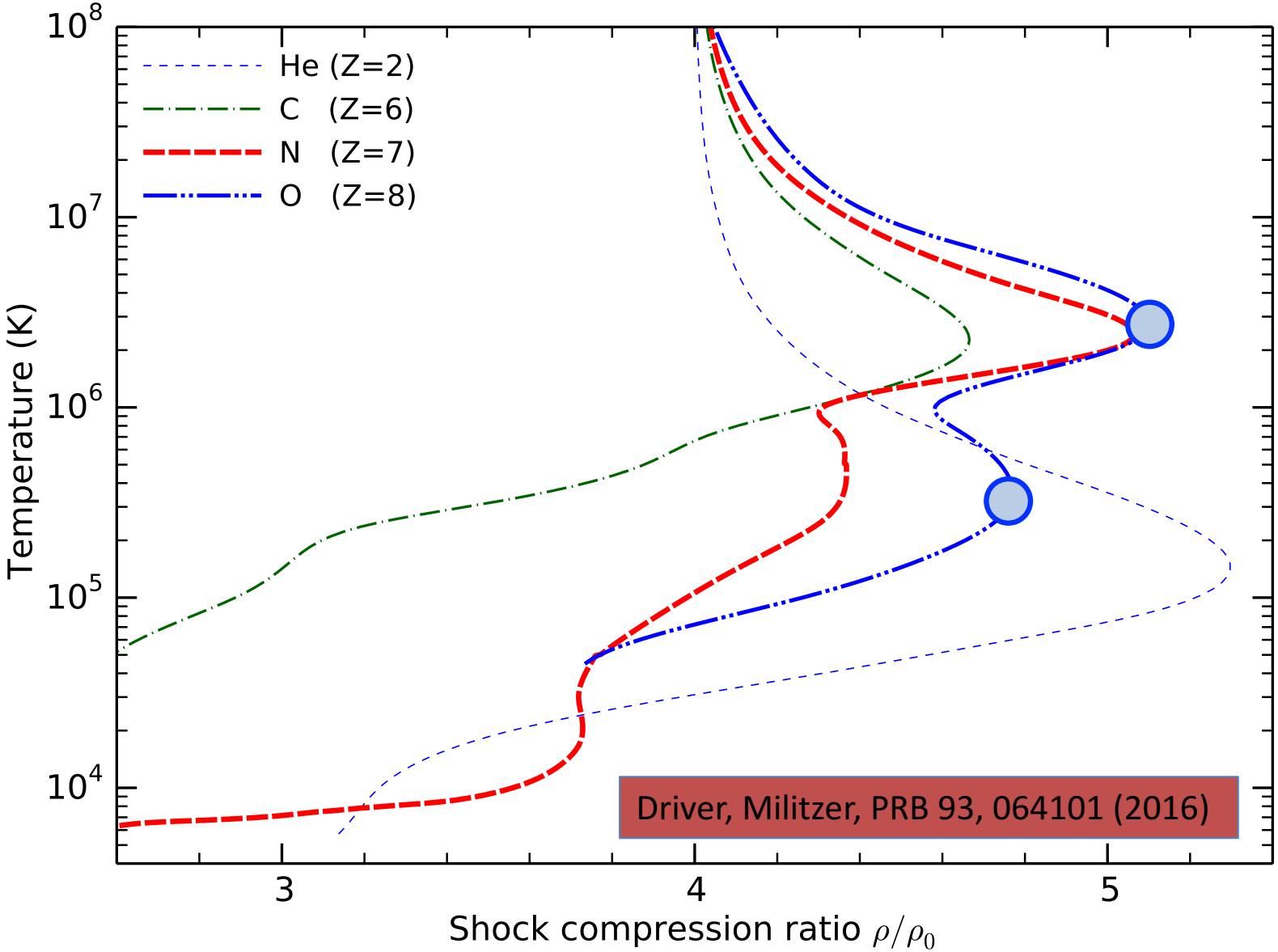

Comparison of Hugoniot Curves for Different Materials

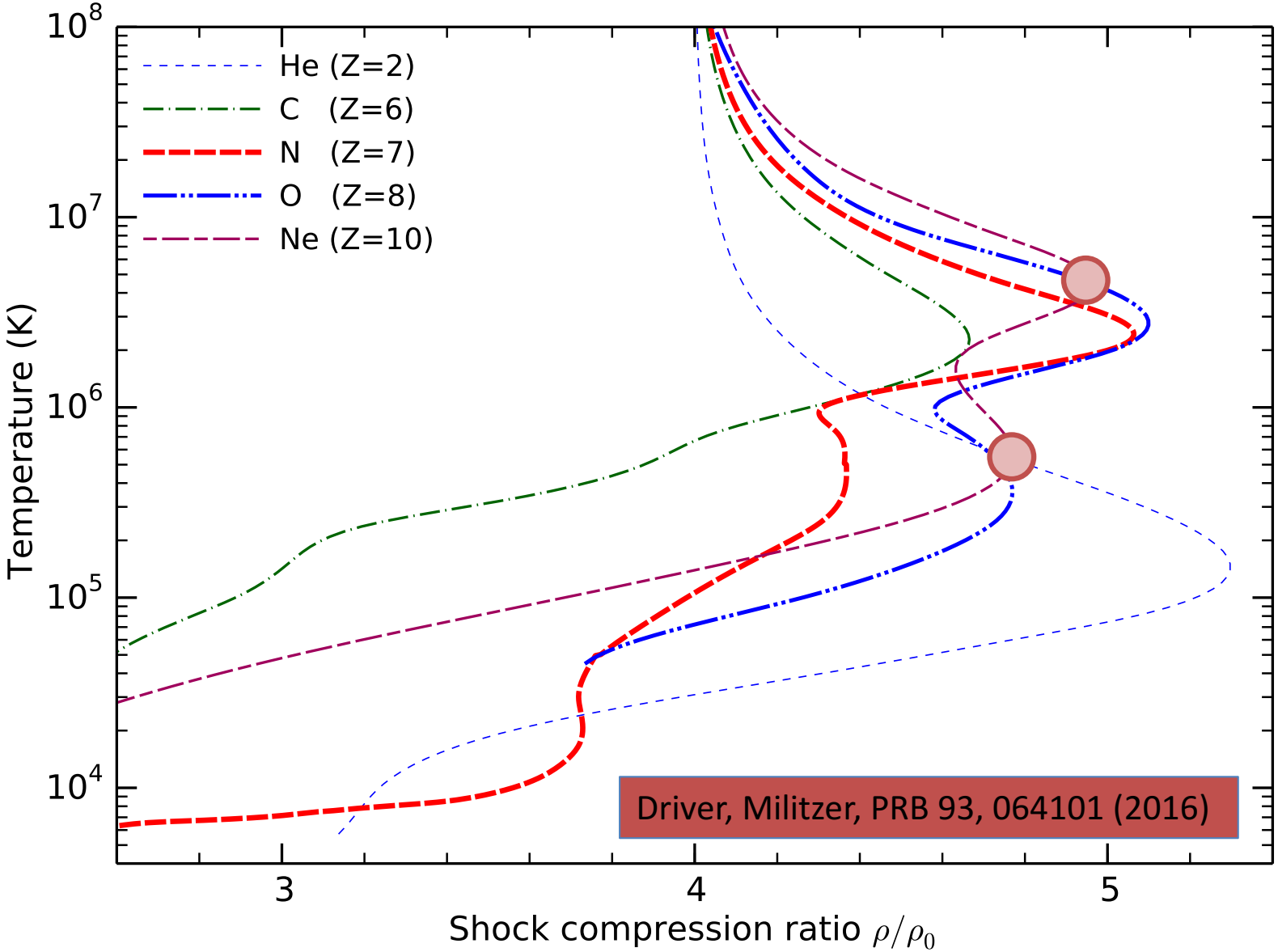

Comparison of Hugoniot Curves for Different Materials

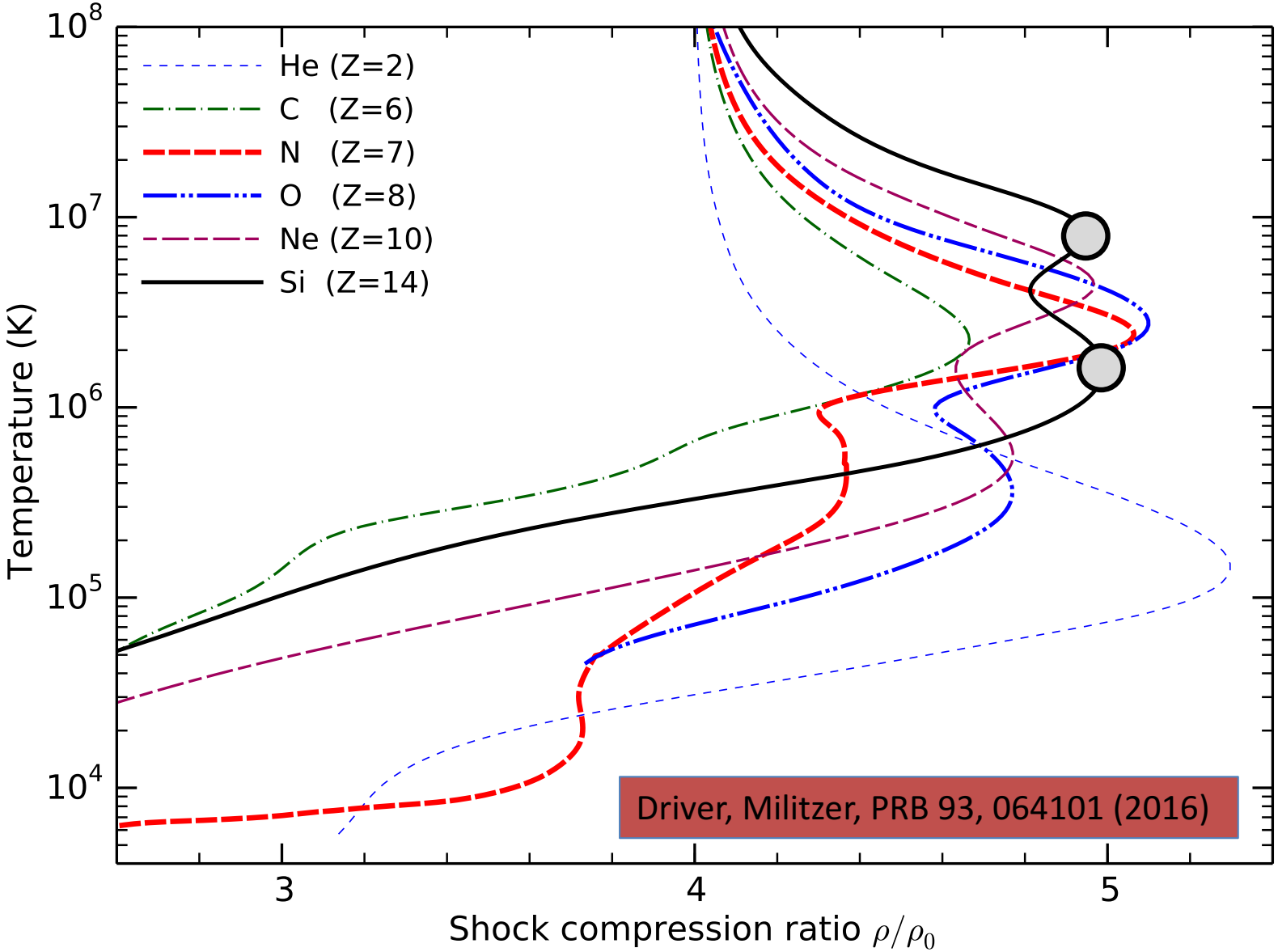

Conclusions

- For elements from hydrogen to through silicon, the energy, pressure, and g(r) functions computed with PIMC and KS-DFT agree well at 2×10^6 K.
- Internal energy agrees to better than 5 Ha/atom. Pressure to 2%.
- So far, we could not detect any problem with the zero-temperature exchange-correlation functionals.
- We will provide more EOS data to improve orbit-free methods.
- Second row elements: More comparison between simulations and experiments
- Extending PIMC to third row elements in particular iron.

The End